pharmaceutics

MDPI

Article

Contribution to the Synthesis, Characterization, Separation and Quantification of New *N*-Acyl Thiourea Derivatives with Antimicrobial and Antioxidant Potential

Roxana Roman [1], Lucia Pintilie [2,*], Diana Camelia Nuță [1], Miron Teodor Căproiu [3], Florea Dumitrașcu [3], Irina Zarafu [4], Petre Ioniță [4], Ioana Cristina Marinaș [5,6], Luminița Mărușescu [6,7], Eleonora Kapronczai [8], Simona Ardelean [9] and Carmen Limban [1]

[1] Department of Pharmaceutical Chemistry, Faculty of Pharmacy, "Carol Davila" University of Medicine and Pharmacy, 6 Traian Vuia, 020956 Bucharest, Romania; roxana.roman@drd.umfcd.ro (R.R.); diana.nuta@umfcd.ro (D.C.N.); carmen.limban@umfcd.ro (C.L.)
[2] National Institute of Chemical-Pharmaceutical Research & Development, 112 Vitan Av., 031299 Bucharest, Romania
[3] "C. D. Nenitzescu" Institute of Organic and Supramolecular Chemistry, 202B Splaiul Independenței, 060023 Bucharest, Romania; dorucaproiu@gmail.com (M.T.C.); fdumitra@yahoo.com (F.D.)
[4] Department of Organic Chemistry, Biochemistry and Catalysis, Faculty of Chemistry, University of Bucharest, 4-12 Regina Elisabeta, 030018 Bucharest, Romania; zarafuirina@yahoo.fr (I.Z.); p_ionita@yahoo.co.uk (P.I.)
[5] Research Institute of the University of Bucharest, University of Bucharest, 90 Panduri Road, 030018 Bucharest, Romania; ioana.cristina.marinas@gmail.com
[6] Sanimed International Impex S.R.L., 087040 Calugareni, Romania; lumi.marutescu@gmail.com
[7] Department of Microbiology and Immunology, Faculty of Biology, University of Bucharest, 91-96 Splaiul Independenței, 060101 Bucharest, Romania
[8] Supramolecular Organic and Organometallic Chemistry Centre, Department of Chemistry, Faculty of Chemistry and Chemical Engineering, Babeş-Bolyai University, 11 Arany János, 400028 Cluj-Napoca, Romania
[9] Department of Pharmaceutical Technology, Faculty of Pharmacy, "Vasile Goldiș" Western University, 86 Liviu Rebreanu, 310045 Arad, Romania; simonaaardelean@yahoo.com
* Correspondence: lucia.pintilie@gmail.com

Abstract: The present study aimed to synthesize, characterize, and validate a separation and quantification method of new *N*-acyl thiourea derivatives (**1a**–**1o**), incorporating thiazole or pyridine nucleus in the same molecule and showing antimicrobial potential previously predicted in silico. The compounds have been physiochemically characterized by their melting points, IR, NMR and MS spectra. Among the tested compounds, **1a**, **1g**, **1h**, and **1o** were the most active against planktonic *Staphylococcus aureus* and *Pseudomonas aeruginosa*, as revealed by the minimal inhibitory concentration values, while **1e** exhibited the best anti-biofilm activity against *Escherichia coli* (showing the lowest value of minimal inhibitory concentration of biofilm development). The total antioxidant activity (TAC) assessed by the DPPH method, evidenced the highest values for the compound **1i,** followed by **1a**. A routine quality control method for the separation of highly related compounds bearing a chlorine atom on the molecular backbone (**1g**, **1h**, **1i**, **1j**, **1m**, **1n**) has been developed and validated by reversed-phase high-performance liquid chromatography (RP—HPLC), the results being satisfactory for all validation parameters recommended by the ICH guidelines (i.e., system suitability, specificity, the limits of detection and quantification, linearity, precision, accuracy and robustness) and recommending it for routine separation of these highly similar compounds.

Keywords: *N*-acyl thiourea derivatives; antimicrobial; antibiofilm; antioxidant activity; validation; HPLC; ICH

Citation: Roman, R.; Pintilie, L.; Nuță, D.C.; Căproiu, M.T.; Dumitrașcu, F.; Zarafu, I.; Ioniță, P.; Marinaș, I.C.; Mărușescu, L.; Kapronczai, E.; et al. Contribution to the Synthesis, Characterization, Separation and Quantification of New *N*-Acyl Thiourea Derivatives with Antimicrobial and Antioxidant Potential. *Pharmaceutics* **2023**, *15*, 2501. https://doi.org/10.3390/pharmaceutics15102501

Academic Editors: Alessio Soggiu, Gabriele Meroni and Piera Anna Martino

Received: 19 August 2023
Revised: 8 October 2023
Accepted: 17 October 2023
Published: 20 October 2023

1. Introduction

Many heterocyclic compounds containing thiophene, pyrazole, thiazolidine, *s*-triazine, pyridazine, fluoroquinolone, benzothiazole, benzoxazolone nuclei as well as thiourea moiety have proven to imprint versatile biological activities. They have been reported to

possess antimicrobial [1–6], anticancer [7–9], antiviral [10,11], anti-allergic [12], anticonvulsant [13–17], and antioxidant activities [2,18].

The introduction of atoms, functional groups or other heterocyclic cores to the thiourea pharmacophore structure has been proven to be a beneficial approach for improving some of the desired biological activities. Previous studies have demonstrated that binding of heterocyclic rings to the thiourea moiety lowers the toxicity and increases their potency. In this regard, promising anti-HIV agents were obtained by attaching **1h**-imidazole moiety to thiourea derivatives [19,20]. Also, in a series of new 1-benzoyl, 3-phenyl-thiourea derivatives, *halo*- and *methoxy*-groups substituted on aryl rings displayed increased activity against all tested bacterial strains, compared to the other substituents [21].

Some *N*-(4-*R*-phenyl)/benzyl/(2-phenylethyl)-*N*′-(6-phenylpyridazin-3-yl)thiourea derivatives carrying thiourea group in position 3 were synthesized and evaluated for their antimicrobial activity using a broth microdilution test. These compounds showed promising inhibitory activity against *Staphylococcus aureus* and *Escherichia coli* bacterial strains and antifungal activity against *Candida* sp. [4].

A few thiourea derivatives of (2′-(**1h**-tetrazol-5-yl)biphenyl-4-yl)methanamine demonstrated in vitro antibacterial activity against *Staphylococcus aureus*, *Pseudomonas aeruginosa*, and *Escherichia coli*. These compounds also exhibited important antifungal activity [6].

Novel 2-methylquinazolin-4(3*H*)-one derivatives bearing thiourea functionality in position 3 were synthesized and screened for their antimicrobial and anti-inflammatory (TNF-α and IL-6) activities. Some of the compounds showed moderate antibacterial activities in comparison with ciprofloxacin [22].

New compounds containing thiourea group in position 6 of 3-methyl-2(3*H*)-benzoxazolone and 5-chloro-3-methyl-2(3*H*)-benzoxazolone rings were evaluated and 1-phenyl-3-(5-chloro-3-methyl-2-oxo-3*H*-benzoxazole-6-yl)thiourea and 1-benzyl-3-(5-chloro-3-methyl-2-oxo-3*H*-benzoxazole-6-yl)thiourea exhibited good inhibitory profiles against *Escherichia coli* [23].

New thiourea derivatives of 1,3-thiazole have been synthesized and tested in vitro against Gram-positive cocci, Gram-negative strains, *Candida albicans*, *Mycobacterium tuberculosis* reference (H37Rv), and clinical strains. 1-(3,4-Dichlorophenyl)-3-(1,3-thiazol-2-yl)thiourea and 1-(3-chloro-4-fluorophenyl)-3-(1,3-thiazol-2-yl)thiourea showed a significant inhibitory effect against Gram-positive cocci with MIC values between 2 and 32 μg/mL. The same compounds inhibited the biofilm formation of both methicillin-susceptible and resistant *S. epidermidis* strains. For the antimicrobial activity, the presence of the halogen atom, especially in the third position of the phenyl nucleus is crucial. All these compounds have also proved to be cytotoxic on the MT-4 tumoral cells and exhibited antiviral activity on a large set of DNA and RNA viruses, including Human Immunodeficiency Virus (HIV) type 1 [10].

Inspired by the data collected from the scientific literature and based on the molecular descriptors and molecular docking studies carried out in our previous work [24], the present study aimed to synthesize new *N*-acyl thiourea derivatives (referred to in the current paper as **1a**–**1o**), that incorporate both thiazole or pyridine nuclei in the same molecule. The presence of electron-withdrawing, electron-donating atoms, and specific functional groups on the acyl thiourea moiety's heterocyclic core has been investigated to elucidate their influence on antimicrobial, antibiofilm, and antioxidant activities.

Among the synthesized compounds, six molecules were designed by adding the chlorine atom to the molecular backbone, leading to close structural similarity of the resulting chemical entities. For this reason, a routine quality control method for the separation of the highly related compounds (**1g**, **1h**, **1i**, **1j**, **1m**, **1n**) has been developed and validated through reversed-phase high-performance liquid chromatography method (RP—HPLC).

2. Materials and Methods

2.1. Chemistry

General procedure for the synthesis of the new compounds (**1a**–**1o**):

A solution of ammonium thiocyanate (0.01 mol) in anhydrous acetone (5 mL) was added to a solution of 2-(4-ethylphenoxymethyl)benzoyl chloride (0.01 mol) in anhydrous acetone (15 mL). The reaction mixture was refluxed for one hour. A solution of the primary heterocyclic amine in anhydrous acetone was added to the cooled mixture. Then, the reaction mixture was heated for two hours. The resulting compound was precipitated by pouring it into cold water. The crude substance was purified by crystallization from 2-propanol using charcoal.

The synthesis of the 2-((4-ethylphenoxy)methyl)benzoic acid and 2-((4-ethylphenoxy) methyl)benzoic acid chloride was presented in a previous article [25].

2.2. Measurements

Most of the reagents were used as received from Sigma-Aldrich (St. Louis, MO, USA) and Merck (Darmstadt, Germany). Ammonium thiocyanate was dried at 100 °C, and acetone was dried on calcium chloride and then distilled.

2.2.1. Melting Points

Melting points were recorded by Electrothermal 9100 apparatus (Bibby Scientific Ltd., Stone, UK) and were uncorrected.

2.2.2. Infrared Spectra

The IR spectra were recorded on a Bruker Vertex 70 FT-IR spectrometer (Bruker Corporation, Billerica, MA, USA). Absorptions were reported with the following relative intensities: w—weak band; m—medium band; s—intense band; vs—very intense band.

2.2.3. Nuclear Magnetic Resonance Spectra

1h NMR and ^{13}C NMR spectra were recorded on a Bruker Fourier 300 MHz instrument (Bruker Corporation, Billerica, MA, USA), operating at 300 MHz for **1h** NMR and at 75 MHz for ^{13}C NMR in deuterated dimethyl sulfoxide (DMSO-d6), with tetramethylsilane used as internal standard. Data were reported as follows: a chemical shift in ppm (δ), multiplicity (s = singlet, brs = broad singlet, d = doublet, t = triplet, q = quartet, m= multiplet, dd = double doublet, td = triple doublet, ddd = doublet of doublets), signal/atom attribution, and the coupling constant (Hz). For ^{13}C NMR data, the order is as follows: chemical shifts and signal/atom attribution; Cq = quaternary carbon.

2.2.4. Mass Spectra

The APCI + high-resolution mass spectra (MS) were recorded on a Thermo Scientific LTQ-Orbitrap XL spectrometer with a standard ESI/APCI source. Thermo Xcalibur 4.0 software was used to process the mass spectra (XcaliburTM Software, Thermo Fisher Scientific, 168 3rd Avenue, Waltham, MA USA, www.thermofisher.com).

2.2.5. Spectral Data

2-((4-Ethylphenoxy)methyl)-*N*-((thiazol-2-yl)carbamothioyl)benzamide (**1a**)
(m.p. 125–126.5 °C; yield 72%, 2.86 g)

1h-NMR (DMSO-d6, δ ppm, *J* Hz, T = 303 K): 12.60(brs, 2H, NH); 7.69(dd, **1h**, H-4, 1.4, 7.5); 7.62(dd, **1h**, H-4, 1.4, 7.5); 7.56(td, **1h**, H-5, 7.5, 1.4); 7.52(d, **1h**, H-18, 3.7); 7.46(td, **1h**, H-6, 7.5, 1.4); 7.26(d, **1h**, H-19, 3.7); 7.05(d, 2H, H-11, H-13, 8.6); 6.81(d, 2H, H-10, H-14, 8.6); 5.28(s, 2H, H-8); 2.51(q, 2H, H-15, 7.5); 1.12(t, 3H, H-15′, 7.5) (Figure S14, Supplementary Materials, for **1h**-NMR spectrum)

^{13}C-NMR (DMSO-d6, δ ppm, T = 303 K): 178.05(C-16); 166.72(C-1); 158.17(C-17); 156.23(C-9); 137.53(C-18); 136.21(Cq); 136.05(Cq); 133.06(Cq); 130.78(C-5); 128.54(C-11, C-13); 128.53(C-4); 128.42(C-7); 127.67(C-6); 114.64(C-10, C-14); 113.65(C-19); 67.29(C-8); 27.20(C-15); 15.75(C-15′) (Figure S15, Supplementary Materials, for ^{13}C-NMR spectrum).

FT-IR (ATR in solid, ν cm^{-1}): 3222w; 3111w; 3058w; 2961m; 2914m; 1667s; 1607m; 1576m; 1546vs; 1507vs; 1439m; 1380w; 1280s; 1235vs; 1183m; 1161m; 1129m; 1035s; 892w; 818m; 731m; 702m; 673m; 614w (Figure S44, Supplementary Materials, for IR spectrum).

Chemical Formula: $C_{20}H_{19}N_3O_2S_2$, Exact Mass: 397.09187, HRMS (APCI+, DMSO + MeOH): *m*/*z* calcd for $C_{19}H_{19}N_2O_2S^+$ = 339.11618, found 339.11537 (36%, mass error Δm = −2.42 ppm), calcd for $C_{16}H_5O_2^+$ = 239.10666, found 239.10603 (100%, Δm = −2.63 ppm), calcd for $C_{11h9}N_2OS^+$ = 217.04301, found 217.04246 (78%, Δm = −2.35 ppm).

2-((4-Ethylphenoxy)methyl)-*N*-((pyridin-2yl)carbamothioyl)benzamide (**1b**)

(m.p. 68.3–70.1 °C; yield 81%, 3.17 g)

1h-NMR (DMSO-d6, δ ppm, *J* Hz, T = 303 K): 13.06(s, **1h**, NH, deuterable); 11.99(brs, **1h**, NH, deuterable); 8.74(brs, **1h**, H-21); 8.40(brs, **1h**, H-18); 7.89(td, **1h**, H-19, 6.9, 2.0); 7.65(dd, **1h**, H-4, 1.2, 7.4); 7.60(dd, **1h**, H-7, 1.8, 7.4); 7.57(td, **1h**, H-6, 7.5, 1.2); 7.47(td, **1h**, H-6, 7.5, 1.8); 7.26(td, **1h**, H-20, 6.9, 2.0); 7.03(d, 2H, H-11, H-13, 8.6); 6.87(d, 2H, H-10, H-14, 8.6); 5.28(s, 2H, H-8); 2.47(q, 2H, H-15, 7.5); 1.08(t, 3H, H-15′, 7.5) (Figure S16, Supplementary Materials, for **1h**-NMR spectrum).

^{13}C-NMR (DMSO-d6, δ ppm, T = 303 K): 177.67(C-16); 170.08(C-1); 156.17(C-9); 151.15(Cq); 148.29(C-18); 137.96(C-19); 135.95(Cq); 133.21(Cq); 131.10(C-5); 128.64(C-4); 128.51(C-11, C-13); 128.39(C-7); 127.71(C-6); 121.22(C-20); 115.37(CH); 114.55(C-10, C-14); 67.44(C-8); 27.20(C-15); 15.69(C-15′) (Figure S17, Supplementary Materials, for ^{13}C-NMR spectrum).

FT-IR (ATR in solid, ν cm^{-1}): 3457m; 3236w; 3030m; 2958m; 2921m; 2861w; 1674m; 1612m; 1576m; 1514vs; 1456s; 1433s; 1387m; 1327s; 1290s; 1240vs; 1155s; 1030m; 838w; 812m; 779m; 734m; 688m; 655w (Figure S45, Supplementary Materials, for IR spectrum).

Chemical Formula: $C_{22}H_{21}3NO_2S$, Exact Mass: 391.13545, HRMS (APCI+, DMSO + MeOH): *m*/*z* calcd for $[M + H]^+$ $C_{22}H_{22}N_3O_2S^+$ = 392.14272, found 392.14171 (100%, Δm = −2.58 ppm) calcd for $[M-H]^+$ $C_{22}H_{20}N_3O_2S^+$ = 390.12707, found 390.12683 (84%, Δm = −0.62 ppm), calcd for $C_{16}H_{18}NO_2^+$ = 256.13321, found 256.13301 (41%, Δm = −0.78 ppm), calcd for $C_{16}H_{15}O_2^+$ = 239.10666, found 239.10655 (74%, Δm = −0.46 ppm), calcd for $C_8H_8NO^+$ = 134.06004, found 134.06000 (6%, Δm = −0.30 ppm).

2-((4-Ethylphenoxy)methyl)-*N*-((pyridin-3-yl)carbamothioyl)benzamide (**1c**)

(m.p. 157.6–159 °C; yield 63%, 2.46 g)

1h-NMR (DMSO-d6, δ ppm, *J* Hz): 12.32(s, **1h**, NH, deuterable); 11.97(brs, **1h**, NH, deuterable); 8.63(d, **1h**, H-21, 2.3); 8.44(dd, **1h**, H-20, 1.6, 4.8); 8.01(ddd, **1h**, H-18, 1.6, 2.3, 8.3); 7.63(dd, **1h**, H-4, 1.2, 7.4); 7.60(dd, **1h**, H-7, 1.8, 7.4); 7.57(td, **1h**, H-6, 7.5, 1.2); 7.47(td, **1h**, H-6, 7.5, 1.8); 7.44(dd, **1h**, H-19, 4.6, 8.3); 7.09(d, 2H, H-11, H-13, 8.6); 6.90(d, 2H, H-10, H-14, 8.6); 5.28(s, 2H, H-8); 2.51(q, 2H, H-15, 7.5); 1.12(t, 3H, H-15′, 7.5) (Figure S18, Supplementary Materials, for **1h**-NMR spectrum).

^{13}C-NMR (DMSO-d6, δ ppm): 180.23(C-16); 169.99(C-1); 156.27(C-9); 147.00(C-20); 146.14(C-21); 136.20(Cq); 135.84(Cq); 134.87(Cq); 133.25(Cq); 132.41(C-18); 131.02(C-5); 128.57(C-11, C-13); 128.45(C-4); 128.34(C-7); 127.71(C-6); 123.25(C-18); 114.55(C-10, C-14); 67.47(C-8); 27.23(C-15); 15.76(C-15′) (Figure S19, Supplementary Materials, for ^{13}C-NMR spectrum).

FT-IR (ATR in solid, ν cm^{-1}): 3128w; 3032w; 2956m; 2912m; 2868m; 1673m; 1530vs; 1510vs; 1382m; 1284m; 1233s; 1199m; 1168s; 1120m; 1029m; 881w; 821m; 746s; 707m; 675m; 648w; 603w (Figure S46, Supplementary Materials, for IR spectrum).

Chemical Formula: $C_{22}H_{21}N_3O_2S$, Exact Mass: 391.13545, HRMS (APCI+, DMSO + MeOH): *m*/*z* calcd for $[M + H]^+$ $C_{22}H_{22}N_3O_2S^+$ = 392.14272, found 392.14227 (100%, Δm = −1.15 ppm), calcd for $[M - S - H]^+$ $C_{22}H_{20}N_3O_2^+$ = 358.15500, found 358.15497 (4%, Δm = −0.08 ppm), calcd for $C_{16}H_{18}NO_2^+$ = 256.13321, found 256.13303 (12%, Δm = −0.70 ppm), calcd for $C_{16}H_{15}O_2^+$ = 239.10666, found 239.10638 (38%, Δm = −1.17 ppm), calcd for $C_6H_5N_2S^+$ = 137.01680, found 137.01651 (6%, Δm = −2.12 ppm), calcd for $C_8H_8NO^+$ = 134.06004, found 134.05977 (8%, Δm = −2.01 ppm).

2-((4-Ethylphenoxy)methyl)-*N*-((3-methylpyridin-2-yl)carbamothioyl)benzamide (**1d**)

(m.p. 112–113.3 °C; yield 71%, 2.88 g)

1h-NMR (DMSO-d6, δ ppm, *J* Hz): 12.11(s, **1h**, NH, deuterable); 11.94(brs, **1h**, NH, deuterable); 8.31(dd, **1h**, H-21, 4.5, 1.3); 7.73(dd, **1h**, H-19, 1.3, 7.6); 7.63(dd, **1h**, H-4, 1.2, 7.4); 7.60(dd, **1h**, H-7, 1.8, 7.4); 7.57(td, **1h**, H-5, 7.5, 1.2); 7.47(td, **1h**, H-6, 7.5, 1.8); 7.30(dd, **1h**, H-20, 4.5, 7.6); 7.09(d, 2H, H-11, H-13, 8.6); 6.89(d, 2H, H-10, H-14, 8.6); 5.27(s, 2H, H-8); 3.31(s, 3H, H-18′); 2.51(q, 2H, H-15, 7.5); 1.14(t, 3H, H-15′, 7.5) (Figure S20, Supplementary Materials, for **1h**-NMR spectrum).

^{13}C-NMR (DMSO-d6, δ ppm): 180.02(C-16); 169.87(C-1); 156.21(C-9); 150.04(C-17); 146.15(C-C-21); 133.39(C-19); 136.18(Cq); 135.78(Cq); 133.34(Cq); 130.99(C-5); 130.53(Cq); 128.64(C-4); 128.59(C-11, C-13); 128.53(C-7); 127.74(C-6); 123.20(C-20); 114.66(C-10, C-14); 67.48(C-8); 27.24(C-15); 17.03(C-18′); 15.77(C-15′) (Figure S21, Supplementary Materials, for ^{13}C-NMR spectrum).

FT-IR (ATR in solid, ν cm^{-1}): 3149m; 3062w; 2960m; 2929m; 2870m; 1672s; 1604w; 1581w; 1504vs; 1454vs; 1373m; 1326m; 1235s; 1161s; 1114m; 1019m; 954w; 882w; 816w; 734m; 667m; 582w (Figure S47, Supplementary Materials, for IR spectrum).

Chemical Formula: $C_{23}H_{23}N_3O_2S$, Exact Mass: 405.15110, HRMS (APCI+, DMSO + MeOH): *m*/*z* calcd for $[M + H]^+$ $C_{23}H_{24}N_3O_2S^+$ = 406.15837, found 406.15779 (31%, Δm = −1.43 ppm), calcd for $[M - H]^+$ $C_{23}H_{22}N_3O_2S^+$ = 404.14272, found 404.14235 (47%, Δm = −0.92 ppm), calcd for $C_{16}H_{18}NO_2^+$ = 256.13321, found 256.13296 (21%, Δm = −0.98 ppm), calcd for $C_{16}H_{15}O_2^+$ = 239.10666, found 239.10636 (100%, Δm = −1.25 ppm), calcd for $C_7H_7N_2S^+$ = 151.03245, found 151.03220 (28%, Δm = −1.66 ppm), calcd for $C_8H_8NO^+$ = 134.06004, found 134.05982 (22%, Δm = −1.64 ppm).

2-((4-Ethylphenoxy)methyl)-*N*-((4-methylpyridin-2-yl)carbamothioyl)benzamide (**1e**) (m.p. 92.6–93.9 °C; yield 68%, 2.76 g)

1h-NMR (DMSO-d6, δ ppm, *J* Hz): 13.01(s, **1h**, NH, deuterable); 11.94(brs, **1h**, NH, deuterable); 8.60(brs, **1h**, H-18); 8.24(brs, **1h**, H-21); 7.63(dd, **1h**, H-4, 1.2, 7.4); 7.60(dd, **1h**, H-7, 1.8, 7.4); 7.57(td, **1h**, H-5, 7.5, 1.2); 7.47(td, **1h**, H-6, 7.5, 1.8); 7.10(brs, **1h**, H-20); 7.09(d, 2H, H-11, H-13, 8.6); 6.89(d, 2H, H-10, H-14, 8.6); 5.27(s, 2H, H-8); 2.49(q, 2H, H-15, 7.5); 2.36(s, 3H, H-19′); 1.09(t, 3H, H-15′, 7.5) (Figure S22, Supplementary Materials, for **1h**-NMR spectrum).

The formation of hydrogen bonds inhibits the free rotation around the SC–N–C[17] bond and instead, the protons in the pyridine ring are on the time scale of the NMR experiment. By heating to 70 °C, the respective signals become sharper and present a hyperfine structure. The signals of carbon atoms in the pyridine ring appear broadened for the same reason.

^{13}C-NMR (DMSO-d6, δ ppm): 177.52(C-16); 170.14(brs, C-1); 156.16(C-9); 151.28(C-17); 148.93(C-19); 147.90(C-21); 136.11(Cq); 135.92(Cq); 133.26(Cq); 131.08(C-5); 128.51(C-7); 128.50(C-11, C-13); 128.39(C-4); 127.71(C-6); 122.18(C-20); 115.79(C-18); 114.54(C-10, C-14); 67.42(C-8); 27.18(C-15); 20.88(C-19′); 15.67(C-15′) (Figure S23, Supplementary Materials, for ^{13}C-NMR spectrum).

FT-IR (ATR in solid, ν cm^{-1}): 3348w; 3162w; 3035w; 2968w; 2922w; 2872w; 1675m; 1606m; 1507vs; 1446m; 1378m; 1326s; 1289m; 1225s; 1151s; 1026m; 897w; 828m; 793w; 735m; 668m; 596w (Figure S48, Supplementary Materials, for IR spectrum).

Chemical Formula: $C_{23}H_{23}N_3O_2S$, Exact Mass: 405.15110, HRMS (APCI+, DMSO + MeOH): *m*/*z* calcd for $[M + H]^+$ $C_{23}H_{24}N_3O_2S^+$ = 406.15837, found 406.15710 (100%, Δm = −3.13 ppm), calcd for $[M - H]^+$ $C_{23}H_{22}N_3O_2S^+$ = 404.14272, found 404.14241 (8%, Δm = −0.78 ppm), calcd for $C_{16}H_{18}NO_2^+$ = 256.13321, found 256.13269 (2%, Δm = −2.03 ppm), calcd for $C_{16}H_{15}O_2^+$ = 239.10666, found 239.10630 (6%, Δm = −1.51 ppm), calcd for $C_7H_7N_2S^+$ = 151.03245, found 151.03225 (2%, Δm = −1.32 ppm).

2-((4-Ethylphenoxy)methyl)-*N*-((5-methylpyridin-2-yl)carbamothioyl)benzamide (**1f**) (m.p. 128–129.3 °C; yield 85%, 3.44 g)

1h-NMR (DMSO-d6, δ ppm, *J* Hz, T = 333 K): 12.86(s, **1h**, NH, deuterable); 11.82(brs, **1h**, NH, deuterable); 8.54(brs, **1h**, H-18); 8.23(brs, **1h**, H-21); 7.77(dd, **1h**, H-19, 1.9, 8.6); 7.65(dd, **1h**, H-4, 1.2, 7.4); 7.60(dd, **1h**, H-7, 1.8, 7.4); 7.57(td, **1h**, H-5, 7.5, 1.2); 7.47(td, **1h**, H-6, 7.5, 1.8); 7.05(d, 2H, H-11, H-13, 8.6); 6.88(d, 2H, H-10, H-14, 8.6); 5.28(s, 2H, H-8);

2.49(q, 2H, H-15, 7.5); 2.30(s, 3H, H-20′); 1.11(t, 3H, H-15′, 7.5) (Figure S24, Supplementary Materials, for **1h**-NMR spectrum).

At 30 °C, the spectrum is composed of broad lines, and we preferred the temperature of 60 °C for simulating the molecular movement.

^{13}C-NMR (DMSO-d6, δ ppm, T = 333 K): 177.47(C-16); 169.86(brs, C-1); 156.24(C-9); 149.05(Cq); 148.03(C-21); 138.15(C-19); 136.21(Cq); 135.94(Cq); 133.32(Cq); 131.03(C-5); 130.52(Cq); 128.46(C-7); 128.41(C-4); 128.38(C-11, C-13); 127.66(C-6); 115.09(C-18); 114.70(C-10, C-14); 67.56(C-8); 27.16(C-15); 17.27(C-20′); 15.52(C-15′) (Figure S25, Supplementary Materials, for ^{13}C-NMR spectrum).

FT-IR (ATR in solid, ν cm^{-1}): 3237s; 3040m; 2963m; 2929m; 2869m; 1661m; 1605w; 1580m; 1526vs; 1471s; 1382m; 1344s; 1291m; 1248m; 1213s; 1149s; 1078w; 1047w; 1014m; 961w; 898w; 823w; 783m; 756m; 724m; 642w; 614w (Figure S49, Supplementary Materials, for IR spectrum).

Chemical Formula: $C_{23}H_{23}N_3O_2S$, Exact Mass: 405.15110, HRMS (APCI+, DMSO + MeOH): *m*/*z* calcd for $[M + H]^+$ $C_{23}H_{24}N_3O_2S^+$ = 406.15837, found 406.15724 (100%, Δm = −2.78 ppm), calcd for $C_{16}H_{18}NO_2^+$ = 256.13321, found 256.13262 (3%, Δm = −2.30 ppm), calcd for $C_{16}H_{15}O_2^+$ = 239.10666, found 239.10710 (10%, Δm = 1.84 ppm), calcd for $C_7H_7N_2S^+$ = 151.03245, found 151.03261 (6%, Δm = 1.06 ppm).

2-((4-Ethylphenoxy)methyl)-*N*-((5-chloropyridin-2-yl)carbamothioyl)benzamide (**1g**) (m.p. 135.7–136.9 °C; yield 74%, 3.15 g)

1h-NMR (DMSO-d6, δ ppm, *J* Hz, T = 303 K): 13.08(s, **1h**, NH, deuterable); 12.13(brs, **1h**, NH, deuterable); 8.76(brs, **1h**, H-18); 8.45(d, **1h**, H-21, 2.4); 8.03(dd, **1h**, H-19, 2.4, 9.0); 7.65(dd, **1h**, H-4, 1.2, 7.4); 7.60(dd, **1h**, H-7, 1.8, 7.4); 7.57(td, **1h**, H-5, 7.5, 1.2); 7.47(td, **1h**, H-6, 7.5, 1.8); 7.03(d, 2H, H-11, H-13, 8.6); 6.86(d, 2H, H-10, H-14, 8.6); 5.27(s, 2H, H-8); 2.47(q, 2H, H-15, 7.5); 1.08(t, 3H, H-15′, 7.5) (Figure S26, Supplementary Materials, for **1h**-NMR spectrum).

^{13}C-NMR (DMSO-d6, δ ppm, T = 303 K): 177.83(C-16); 170.23(brs, C-1); 156.15(C-9); 148.68(Cq); 146.75(C-21); 137.62(C-19); 136.11(Cq); 135.91(Cq); 133.09(Cq); 131.10(C-5); 130.52(Cq); 128.48(C-7); 128.47(C-11, C-13); 128.46(C-4); 128.35(C-6); 116.38(C-18); 114.49(C-10, C-14); 67.41(C-8); 27.17(C-15); 15.66(C-15′) (Figure S27, Supplementary Materials, for ^{13}C-NMR spectrum).

FT-IR (ATR in solid, ν cm^{-1}): 3168m; 3027m; 2963m; 2926m; 2863m; 1675m; 1508vs; 1447s; 1379m; 1327s; 1293m; 1246s; 1219s; 1149s; 1106m; 1028m; 956m; 925w; 860m; 767m; 723m; 662m; 624w (Figure S50, Supplementary Materials, for IR spectrum).

Chemical Formula: $C_{22}H_{20}ClN_3O_2S$, Exact Mass: 425.09648, HRMS (APCI+, DMSO + MeOH): *m*/*z* calcd for $[M + H]^+$ $C_{22}H_{21}ClN_3O_2S^+$ = 426.10375, found 426.10380 (100%, Δm = 0.12 ppm), calcd for $C_{16}H_{18}NO_2^+$ = 256.13321, found 256.13355 (24%, Δm = 1.33 ppm), calcd for $C_{16}H_{15}O_2^+$ = 239.10666, found 239.10708 (88%, Δm = 1.76 ppm), calcd for $C_8H_8NO^+$ = 134.06004, found 134.06022 (9%, Δm = 1.34 ppm).

2-((4-Ethylphenoxy)methyl)-*N*-((2-chloropyridin-3-yl)carbamothioyl)benzamide (**1h**) (m.p. 133.6–134.9 °C; yield 72%, 3.06 g)

1h-NMR (DMSO-d6, δ ppm, *J* Hz, T= 303 K): 12.52(s, **1h**, NH, deuterable); 12.16(brs, **1h**, NH, deuterable); 8.40(dd, **1h**, H-21, 1.8, 8.0); 8.32(dd, **1h**, H-19, 1.8, 4.7); 7.65(dd, **1h**, H-4, 1.2, 7.4); 7.60(dd, **1h**, H-7, 1.8, 7.4); 7.57(td, **1h**, H-5, 7.5, 1.2); 7.50(dd, **1h**, H-20, 4.7, 8.0); 7.47(td, **1h**, H-6, 7.5, 1.8); 7.08(d, 2H, H-11, H-13, 8.6); 6.90(d, 2H, H-10, H-14, 8.6); 5.28(s, 2H, H-8); 2.51(q, 2H, H-15, 7.5); 1.12(t, 3H, H-15′, 7.5) (Figure S28, Supplementary Materials, for **1h**-NMR spectrum).

^{13}C-NMR (DMSO-d6, δ ppm, T = 303 K): 180.26(C-16); 170.28(C-1); 156.20(C-9); 147.05(C-19); 145.27(Cq); 136.29(C-21); 136.17(Cq); 135.81(Cq); 133.14(Cq); 132.57(Cq); 131.07(C-5); 128.51(C-4, C-7, C-11, C-13); 127.76(C-6); 122.93(C-20); 114.54(C-10, C-14); 67.52(C-8); 27.21(C-15); 15.75(C-15′) (Figure S29, Supplementary Materials, for ^{13}C-NMR spectrum).

FT-IR (ATR in solid, ν cm^{-1}): 3098w; 3006m; 2962m; 2931m; 1672m; 1590m; 1516vs; 1451s; 1404m; 1380w; 1325m; 1302m; 1269m; 1245s; 1213m; 1157vs; 1119m; 1064m; 1010m;

951w; 870w; 823w; 755s; 730m; 662w; 640w (Figure S51, Supplementary Materials, for IR spectrum).

Chemical Formula: $C_{22}H_{20}ClN_3O_2S$, Exact Mass: 425.09648, HRMS (APCI+, DMSO + MeOH): *m*/*z* calcd for $[M + H]^+$ $C_{22}H_{21}ClN_3O_2S^+$ = 426.10375, found 426.10289 (4%, Δm = −2.02 ppm), calcd for $[M - Cl]^+$ $C_{22}H_{20}N_3O_2S^+$ = 390.12707, found 390.12641 (100%, Δm = −1.69 ppm), calcd for $C_{17}H_{18}NO_2^+$ = 268.05391, found 268.05347 (7%, Δm = −1.64 ppm), calcd for $C_{16}H_{18}NO_2^+$ = 256.13321, found 256.13290 (3%, Δm = −1.21 ppm), calcd for $C_{16}H_{15}O_2^+$ = 239.10666, found 239.10637 (13%, Δm = −1.21 ppm).

2-((4-Ethylphenoxy)methyl)-*N*-((2-chloropyridin-4-yl)carbamothioyl)benzamide (**1i**) (m.p. 146.1–147.3 °C; yield 65%, 2.76 g)

^{1h}-NMR (DMSO-d6, δ ppm, *J* Hz, T = 303 K): 12.64(s, **1h**, NH, deuterable); 12.11(brs, **1h**, NH, deuterable); 8.38(d, **1h**, H-20, 5.6); 8.08(d, **1h**, H-18, 1.9); 7.71(dd, **1h**, H-21, 1.9, 5.6); 7.62(dd, **1h**, H-7, 1.8, 7.4); 7.58(dd, **1h**, H-7, 1.2, 7.5); 7.57(td, **1h**, H-5, 7.5, 1.2); 7.47(td, **1h**, H-6, 7.5, 1.8); 7.05(d, 2H, H-11, H-13, 8.6); 6.87(d, 2H, H-10, H-14, 8.6); 5.27(s, 2H, H-8); 2.49(q, 2H, H-15, 7.5); 1.10(t, 3H, H-15′, 7.5) (Figure S30, Supplementary Materials, for ^{1h}-NMR spectrum).

^{13}C-NMR (DMSO-d6, δ ppm, T = 303 K): 179.20(C-16); 169.24(C-1); 156.22(C-9); 150.42(C-19); 150.17(C-20); 147.52(Cq); 136.16(Cq); 135.96(Cq); 132.99(Cq); 131.16(C-5); 128.52(C-11, C-13); 128.48(C-4); 128.33(C-7); 127.71(C-6); 116.48(C-21); 116.44(C-18); 114.48(C-10, C-14); 67.41(C-8); 27.19(C-15); 15.69(C-15′) (Figure S31, Supplementary Materials, for ^{13}C-NMR spectrum).

FT-IR (ATR in solid, ν cm^{-1}): 3334w; 3112w; 2954m; 2926m; 2868w; 1682m; 1574s; 1506vs; 1447m; 1378m; 1320m; 1293m; 1224s; 1145s; 1074w; 1056w; 1022m; 982m; 875w; 860w; 831m; 779w; 730m; 676m (Figure S52, Supplementary Materials, for IR spectrum).

Chemical Formula: $C_{22}H_{20}ClN_3O_2S$, Exact Mass 425.09648, HRMS (APCI+, DMSO + MeOH): *m*/*z* calcd for $[M + H]^+$ $C_{22}H_{21}ClN_3O_2S^+$ = 426.10375, found 426.10331 (100%, Δm = −1.03 ppm), calcd for $C_{16}H_{18}NO_2^+$ = 256.13321, found 256.13294 (4%, Δm = −1.05 ppm), calcd for $[C_{16}H_{15}O_2]^+$ = 239.10666, found 239.10626 (20%, Δm = −1.67 ppm).

2-((4-Ethylphenoxy)methyl)-*N*-((6-chloropyridin-3-yl)carbamothioyl)benzamide (**1j**) (m.p. 149.3–150.5 °C; yield 78%, 3.32 g)

^{1h}-NMR (DMSO-d6, δ ppm, *J* Hz, T=303 K): 12.30(s, **1h**, NH, deuterable); 12.04(brs, **1h**, NH, deuterable); 8.48(d, **1h**, H-21, 2.5); 8.09(dd, **1h**, H-18, 2.5, 8.6); 7.55(d, **1h**, H-19, 8.6); 7.62(dd, **1h**, H-7, 1.8, 7.4); 7.58(dd, **1h**, H-7, 1.2, 7.5); 7.57(td, **1h**, H-5, 7.5, 1.2); 7.47(td, **1h**, H-6, 7.5, 1.8); 7.05(d, 2H, H-11, H-13, 8.6); 6.87(d, 2H, H-10, H-14, 8.6); 5.28(s, 2H, H-8); 2.51(q, 2H, H-15, 7.5); 1.12(t, 3H, H-15′, 7.5) (Figure S32, Supplementary Materials, for ^{1h}-NMR spectrum).

^{13}C-NMR (DMSO-d6, δ ppm, T = 303 K): 180.40(C-16); 169.89(C-1); 156.25(C-9); 146.82(C-20); 146.25(C-21); 136.21(C-18); 136.20(Cq); 135.88(C-q); 134.54(Cq); 133.15(Cq); 131.07(C-5); 128.56(C-11, C-13); 128.45(C-4); 128.34(C-7); 127.70(C-6); 123.74(C-19); 114.55(C-10, C-14); 67.44(C-8); 27.22(C-15); 15.76(C-15′) (Figure S33, Supplementary Materials, for ^{13}C-NMR spectrum).

FT-IR (ATR in solid, ν cm^{-1}): 3170s; 3010m; 2958m; 2928m; 2886m; 1752w; 1691s; 1609w; 1574m; 1513vs; 1451s; 1393m; 1314m; 1275m; 1239s; 1166s; 1098m; 1024m; 824m; 735m; 690m; 652w; 608w (Figure S53, Supplementary Materials, for IR spectrum).

Chemical Formula $C_{22}H_{20}ClN_3O_2S$, Exact Mass 425.09648, HRMS (APCI+, DMSO + MeOH): *m*/*z* calcd for $[M + H]^+$ $C_{22}H_{21}ClN_3O_2S^+$ = 426.10375, found 426.10364 (100%, Δm = −0.26 ppm), calcd for $C_{16}H_{18}NO_2^+$ = 256.13321, found 256.13373 (3%, Δm = 2.03 ppm), calcd for $C_{16}H_{15}O_2^+$ = 239.10666, found 239.10722 (14%, Δm = 2.34 ppm).

2-((4-Ethylphenoxy)methyl)-*N*-((5-bromopyridin-2-yl)carbamothioyl)benzamide (**1k**) (m.p. 136.8–138 °C; yield 76%, 3.56 g)

^{1h}-NMR (DMSO-d6, δ ppm, *J* Hz, T = 303 K): 13.07(brs, **1h**, NH, deuterable); 12.14(brs, **1h**, NH, deuterable); 8.71(brs, **1h**, H-18); 8.53(d, **1h**, H-2.3); 8.14(dd, **1h**, H-19, 2.3, 9.0); 7.64(dd, **1h**, H-4, 1.2, 7.4); 7.60(dd, **1h**, H-7, 1.8, 7.4); 7.57(td, **1h**, H-5, 7.5, 1.2); 7.47(td, **1h**, H-6, 7.5, 1.8); 7.03(d, 2H, H-11, H-13, 8.6); 6.86(d, 2H, H-10, H-14, 8.6); 5.27(s, 2H, H-8);

2.47(q, 2H, H-15, 7.5); 1.09(t, 3H, H-15′, 7.5) (Figure S34, Supplementary Materials, for **1h**-NMR spectrum).

^{13}C-NMR (DMSO-d6, δ ppm, T = 303 K): 177.81(C-16); 170.22(C-1); 156.15(C-9); 150.02(Cq); 148.94(C-21); 140.39(C-19); 136.12(Cq); 135.92(Cq); 133.09(Cq); 131.11(C-5); 128.49(C-11, C-13); 128.48(C-7); 128.36(C-4); 127.69(C-6); 116.82(C-18); 115.56(C-20); 114.49(C-10, C-14); 67.41(C-8); 27.18(C-15); 15.68(C-15′) (Figure S35, Supplementary Materials, for ^{13}C-NMR spectrum).

FT-IR (ATR in solid, ν cm^{-1}): 3164m; 3026m; 2961m; 2926m; 2860w; 1674m; 1508vs; 1447s; 1376m; 1326m; 1290m; 1246s; 1220s; 1152s; 1090m; 1027m; 996m; 955w; 926w; 886w; 859w; 824m; 762m; 732s; 658m; 617w (Figure S54, Supplementary Materials, for IR spectrum).

Chemical Formula: $C_{22}H_{20}BrN_3O_2S$, Exact Mass 469.04596, HRMS (APCI+, DMSO + MeOH): *m*/*z* calcd for $[M + H]^+$ $C_{22}H_{21}BrN_3O_2S^+$ = 472.05119, found 472.05057 (74%, Δm = −1.3 ppm), calcd for $C_{16}H_{18}NO_2^+$ = 256.13321, found 256.13312 (50%, Δm = −0.35 ppm), calcd for $C_{16}H_{15}O_2^+$ = 239.10666, found 239.10666 (100%, Δm = 0 ppm), calcd for $C_5H_6BrN_2^+$ = 172.97089, found 172.97096 (6%, Δm = 0.40 ppm), calcd for $C_8H_8NO^+$ = 134.06004, found 134.06001 (10%, Δm = −0.22 ppm), calcd for $[Me_2SO + H]^+$ $C_2H_7SO^+$ = 79.02121, found 79.02091 (4%, Δm = −3.80 ppm).

2-((4-Ethylphenoxy)methyl)-*N*-((6-bromopyridin-2-yl)carbamothioyl)benzamide (**1l**) (m.p. 124.5–125.9 °C; yield 73%, 3.42 g)

1h-NMR (DMSO-d6, δ ppm, *J* Hz, T = 303 K): 12.97(brs, **1h**, NH, deuterable); 12.16(brs, **1h**, NH, deuterable); 8.69(brs, **1h**, H-18); 7.85(t, **1h**, H-19, 7.9); 7.64(dd, **1h**, H-4, 1.2, 7.4); 7.60(dd, **1h**, H-7, 1.8, 7.4); 7.57(td, **1h**, H-5, 7.5, 1.2); 7.51(d, **1h**, H-20, 7.9); 7.47(td, **1h**, H-6, 7.5, 1.8); 7.03(d, 2H, H-11, H-13, 8.6); 6.86(d, 2H, H-10, H-14, 8.6); 5.28(s, 2H, H-8); 2.47(q, 2H, H-15, 7.5); 1.09(t, 3H, H-15′, 7.5) (Figure S36, Supplementary Materials, for **1h**-NMR spectrum).

^{13}C-NMR (DMSO-d6, δ ppm, T = 303 K): 177.98(C-16); 170.11(C-1); 156.16(C-9); 151.18(Cq); 141.03(C-19); 138.73(Cq); 136.13(Cq); 135.97(Cq); 133.02(Cq); 131.01(C-5); 128.53(C-7); 128.50(C-11, C-13); 128.30(C-4); 127.68(C-6); 125.07(C-20); 114.55(C-10, C-14); 114.38(C-18); 67.40(C-8); 27.19(C-15); 15.70(C-15′) (Figure S37, Supplementary Materials, for ^{13}C-NMR spectrum).

FT-IR (ATR in solid, ν cm^{-1}): 3210m; 3172m; 3026m; 2971m; 29286m; 2872w; 1672m; 1556s; 1509vs; 1451m; 1421s; 1322s; 1255m; 1223s; 1170s; 1144m; 1120s; 1069w; 1026m; 980w; 820m; 762m; 725m; 660m (Figure S55, Supplementary Materials, for IR spectrum).

Chemical Formula: $C_{22}H_{20}BrN_3O_2S$, Exact Mass 469.04596, HRMS (APCI+, DMSO + MeOH): *m*/*z* calcd for $[M + H]^+$ $C_{22}H_{21}BrN_3O_2S^+$ = 472.05119, found 472.04990 (100%, Δm = −2.73 ppm), calcd for $C_{16}H_{18}NO_2^+$ = 256.13321, found 256.13287 (4%, Δm = −1.33 ppm), calcd for $C_{16}H_{15}O_2^+$ = 239.10666, found 239.10634 (63%, Δm = −1.34 ppm).

2-((4-Ethylphenoxy)methyl)-*N*-((3,5-dichloropyridin-2-yl)carbamothioyl)benzamide (**1m**) (m.p. 125.1–126.5 °C; yield 64%, 2.94 g)

1h-NMR (DMSO-d6, δ ppm, *J* Hz, T = 303 K): 12.23(s, **1h**, NH, deuterable); 12.09(s, **1h**, NH, deuterable); 8.55(d, **1h**, H-21, 2.3); 8.35(d, **1h**, H-19, 2.3); 7.65(dd, **1h**, H-4, 1.2, 7.4); 7.60(dd, **1h**, H-7, 1.8, 7.4); 7.57(td, **1h**, H-5, 7.5, 1.2); 7.47(td, **1h**, H-6, 7.5, 1.8); 7.09(d, 2H, H-11, H-13, 8.6); 6.90(d, 2H, H-10, H-14, 8.6); 5.26(s, 2H, H-8); 2.52(q, 2H, H-15, 7.5); 1.14(t, 3H, H-15′, 7.5) (Figure S38, Supplementary Materials, for **1h**-NMR spectrum).

^{13}C-NMR (DMSO-d6, δ ppm, T = 303 K): 180.54(C-16); 169.84(C-1); 156.18(C-9); 147.43(Cq); 145.62(C-21); 137.97(C-19); 136.18(Cq); 135.84(Cq); 133.07(Cq); 131.11(C-5); 129.95(Cq); 129.00(Cq); 128.59(C-7); 128.56(C-11, C-13); 128.55(C-4); 127.74(C-6); 114.70(C-10, C-14); 67.45(C-8); 27.25(C-15); 15.79(C-15′) (Figure S39, Supplementary Materials, for ^{13}C-NMR spectrum).

FT-IR (ATR in solid, ν cm^{-1}): 3129m; 3027m; 2962m; 2927m; 2868w; 1671m; 1560m; 1504vs; 1438m; 1231s; 1151s; 1114s; 1050m; 953w; 895w; 853w; 823m; 777m; 743w; 708w; 659w; 610w (Figure S56, Supplementary Materials, for IR spectrum).

Chemical Formula: $C_{22}H_{19}Cl_2N_3O_2S$, Exact Mass 459.05750, HRMS (APCI+, DMSO + MeOH): *m*/*z* calcd for $[M + H]^+$ = $C_{22}H_{20}Cl_2N_3O_2S^+$ 460.06478, found 460.06464 (20%, Δm = −0.30 ppm), calcd for $C_{16}H_{18}NO_2^+$ = 256.13321, found 256.13330 (12%,

Δm = 0.35 ppm), calcd for $C_{16}H_{15}O_2^+$ = 239.10666, found 239.10677 (100%, Δm = 0.46 ppm), calcd for $C_8H_8NO^+$ = 134.06004, found 134.06010 (13%, Δm = 0.45 ppm).

2-((4-Ethylphenoxy)methyl)-*N*-((2,6-dichloropyridin-4-yl)carbamothioyl)benzamide (**1n**) (m.p. 138.6–140 °C; yield 61%, 2.80 g)

^{1h}-NMR (DMSO-d6, δ ppm, *J* Hz, T = 303 K): 12.66(s, **1h**, NH, deuterable); 12.19(s, **1h**, NH, deuterable); 8.01(s, 2H, H-18, H-21); 7.65(dd, **1h**, H-4, 1.2, 7.4); 7.60(dd, **1h**, H-7, 1.8, 7.4); 7.57(td, **1h**, H-5, 7.5, 1.2); 7.47(td, **1h**, H-6, 7.5, 1.8); 7.05(d, 2H, H-11, H-13, 8.6); 6.87(d, 2H, H-10, H-14, 8.6); 5.26(s, 2H, H-8); 2.50(q, 2H, H-15, 7.5); 1.10(t, 3H, H-15′, 7.5) (Figure S40, Supplementary Materials, for ^{1h}-NMR spectrum).

^{13}C-NMR (DMSO-d6, δ ppm, T = 303 K): 179.38(C-16); 169.85(C-1); 156.21(C-9); 149.60(Cq); 149.23(C-20, C-19); 136.16(Cq); 135.99(Cq); 132.910(Cq); 131.22(C-5); 128.50(C-7); 128.49(C-11, C-13); 128.36(C-4); 127.74(C-6); 116.01(C-18, C-21); 114.45(C-10, C-14); 67.39(C-8); 27.18(C-15); 15.68(C-15′) (Figure S41, Supplementary Materials, for ^{13}C-NMR spectrum).

FT-IR (ATR in solid, ν cm^{-1}): 3279m; 3116m; 2958w; 2927m; 2869m; 1681m; 1574s; 1503vs; 1372m; 1296s; 1232s; 1163s; 1123m; 1097m; 1043m; 1002w; 884w; 846w; 820m; 773w; 738w; 678m; 612w (Figure S57, Supplementary Materials, for IR spectrum).

Chemical Formula: $C_{22}H_{19}Cl_2N_3O_2S$, Exact Mass 459.05750, HRMS (APCI+, DMSO + MeOH): *m*/*z* calcd for $[M + H]^+$ $C_{22}H_{20}Cl_2N_3O_2S^+$ = 460.06478, found 460.06400 (100%, Δm = −1.70 ppm), calcd for $[M - S + OH]^+$ $C_{22}H_{20}Cl_2N_3O_3^+$ = 444.08762, found 444.08749 (17%, Δm = −0.29 ppm), calcd for $C_{16}H_{18}NO_2^+$ = 256.13321, found 256.13300 (21%, Δm = −0.82 ppm), calcd for $C_{16}H_{15}O_2^+$ = 239.10666, found 239.10649 (43%, Δm = −0.71 ppm), calcd for $C_5H_5Cl_2N_2^+$ = 162.98243, found 162.98230 (5%, Δm = −0.80 ppm), calcd for $C_8H_8NO^+$ = 134.06004, found 134.05984 (5%, Δm = −1.49 ppm), calcd for $[Me_2SO + H]^+$ $C_2H_7SO^+$ = 79.02121, found 79.02081 (8%, Δm = −5.06 ppm).

2-((4-Ethylphenoxy)methyl)-*N*-((3,5-dibromopyridin-2-yl)carbamothioyl)benzamide (**1o**) (m.p. 140.2–142.9 °C; yield 54%, 2.95 g)

^{1h}-NMR (DMSO-d6, δ ppm, *J* Hz, T = 303 K): 12.24(s, **1h**, NH, deuterable); 12.09(s, **1h**, NH, deuterable); 8.65(d, **1h**, H-21, 2.1); 8.54(d, **1h**, H-19, 2.1); 7.63(dd, **1h**, H-4, 1.2, 7.5); 7.61(dd, **1h**, H-7, 1.8, 7.5); 7.57(td, **1h**, H-5, 7.5, 1.2); 7.48(td, **1h**, H-6, 7.4, 1.8); 7.10(d, 2H, H-11, H-13, 8.6); 6.91(d, 2H, H-10, H-14, 8.6); 5.27(s, 2H, H-8); 2.53(q, 2H, H-15, 7.5); 1.14(t, 3H, H-15′, 7.5) (Figure S42, Supplementary Materials, for ^{1h}-NMR spectrum).

^{13}C-NMR (DMSO-d6, δ ppm, T = 303 K): 180.38(C-16); 169.81(C-1); 156.18(C-9); 148.98(C-17); 148.34(C-21); 143.47(C-19); 136.16(Cq); 135.85(Cq); 133.04(Cq); 131.13(C-5); 128.62(C-7); 128.57(C-11, C-13); 127.75(C-6); 119.54(C-20); 118.52(C-18); 114.70(C-10, C-14); 67.39(C-8); 27.25(C-15); 15.79(C-15′) (Figure S43, Supplementary Materials, for ^{13}C-NMR spectrum).

FT-IR (ATR in solid, ν cm^{-1}): 3130m; 3027w; 2965w; 2844w; 1673m; 1546m; 1504vs; 1430m; 1360m; 1323w; 1236s; 1150vs; 1043m; 952w; 825w; 737m; 696w; 661w (Figure S58, Supplementary Materials, for IR spectrum).

Chemical Formula: $C_{22}H_{19}Br_2N_3O_2S$, Exact Mass 546.95647, HRMS (APCI+, DMSO + MeOH): *m*/*z* calcd for $[M + H]^+$ $C_{22}H_{20}Br_2N_3O_2S^+$ = 549.96170, found 549.96069 (100%, Δm = −1.84 ppm), calcd for $C_{14}H_9BrN_3OS^+$ = 345.96442, found 345.96356 (8%, Δm = −2.49 ppm), calcd for $C_{16}H_{18}NO_2^+$ = 256.13321, found 256.13354 (20%, Δm = 1.29 ppm), calcd for $C_{16}H_{15}O_2^+$ = 239.10666, found 239.10707 (99%, Δm = 7.71 ppm), calcd for $C_8H_8NO^+$ = 134.06004, found 134.06015 (10%, Δm = 0.82 ppm), calcd for $[Me_2SO + H]^+$ $C_2H_7SO^+$ = 79.02121, found 79.02081 (15%, Δm = −5.06 ppm).

2.3. Biological Evaluation of the Antimicrobial Activity

2.3.1. Quantitative Evaluation of the Antimicrobial Activity

The in vitro evaluation of the antimicrobial activity of the compounds was performed using the following standard microbial strains: *Staphylococcus aureus* ATCC 25923, *Enterococcus faecalis* ATCC 29212, *Escherichia coli* ATCC 25922, and *Pseudomonas aeruginosa* ATCC 27853. Fresh microbial cultures grown for 18–24 h on *Plate Count Agar* were used to prepare suspensions in sterile PBS (Phosphate-Buffered Saline). The 0.5 McFarland

standard was used as a reference to adjust the turbidity of the microbial suspensions to 1.5×10^8 colony-forming units (CFU/mL). The compounds were solubilized in DMSO at a stock concentration of 10 mg/mL. Then, serial binary dilutions were prepared in liquid culture medium (Mueller–Hinton) in 96-well plates, starting from 5 mg/mL (the compound testing concentrations were between 5 and 0.009 mg/mL). The medium containing different concentrations of the compounds was further inoculated with the microbial suspensions at a final density of 10^6 CFU/mL. The inoculated 96 well-plates were incubated for 18–24 h at 37 °C. The positive control was represented by ciprofloxacin (5 µg/mL). Growth control was represented by the broth inoculated only with standard microbial suspension. The determinations were performed in triplicate to confirm the MIC (minimum inhibitory concentration) values. The MIC values were determined by visual inspection, as the lowest concentrations of tested compounds that inhibited the microbial growth in the liquid medium (the culture medium remained clear, similar to the sterility control).

2.3.2. Evaluation of the Antibiofilm Activity

The compounds' antibiofilm activity was investigated using the crystal violet microtiter assay. After the determination of the MIC, the 96-well plates were emptied and washed three times with sterile saline to remove non-adherent microbial cells. Microbial cells adhering to the walls of the wells were fixed with 150 µL methanol for 5 min, then stained with 150 µL 1% violet crystal solution (prepared in distilled water) for 20 min. The dye was removed, and the plates were washed using sterile saline. The microbial biofilms formed on the inert substrate were suspended in 33% acetic acid, then the absorbance was read at a wavelength of 490 nm. The minimum inhibitory concentration of the total biofilm mass development (MBIC) was defined as the lowest concentration of compound that induced a decrease in the stained biofilm mass and, consequently, of the absorbance value, at levels similar to those of the sterility control.

2.4. Total Antioxidant Activity (TAC)

A solution of 2,2-diphenyl-1-picrylhydrazyl (DPPH) with a concentration of 4×10^{-4} M in acetone was prepared. Ascorbic acid was used as a reference. Stock solutions of ascorbic acid and compounds **1a**–**1o** were prepared in acetone at a standard concentration of 2 mg/mL. For TAC measurements, 1 mL of stock solution of DPPH was added to 1 mL of stock solution of each compound, and the mixture was kept for 30 min in the dark, followed by the absorbance measuring at 517 nm. A UVD-3500 UV-Vis spectrophotometer was used for this purpose. The TAC percentage was calculated by Equation (1):

$$\text{TAC}, \% = \frac{\text{Abs}_\text{i} - \text{Abs}_{30\text{min}}}{\text{Abs}_\text{i}} \times 100 \quad (1)$$

where Abs_i is the initial absorbance of the mixture, and the $\text{Abs}_{30\,\text{min}}$ is the absorbance measured after 30 min [26–28].

2.5. RP—HPLC Analytical Method

2.5.1. Materials and Equipment

HPLC grade solvents were used in the HPLC analysis: acetonitrile reagent (Fischer Scientific, Waltham, MA, USA), methanol reagent (Scharlau, Hamburg Germany), triethylamine (Sigma-Aldrich, Munich, Germany), and orthophosphoric acid (Fisher Scientific, Waltham, MA, USA).

The Waters Alliance HPLC system, comprised of the following modules: 2695 + 2998 separation module, 998 PDA detector, and PC equipped with "Empower no. 3 PDA Software", was used for the determination. The samples were weighed by using a Mettler Toledo analytical balance, and the pH of the solutions was determined with a pH meter inoLab pH7310P. To filter the solutions injected in the HPLC system, syringe nylon filters (0.45 µm) (Agilent Technologies, Santa Clara, CA, USA) were used.

2.5.2. Chromatographic Conditions

The RP-HPLC analytical method was developed and optimized by using a chromatographic column with a stationary phase composed of octadecyl silica gel (C18), 250 mm length, 4.6 mm diameter, and particle size of 5 µm (Inertsil ODS-3, 5 µm, 250 × 4.6 mm). The chosen column and the samples were maintained at room temperature during the determinations.

The mobile phase, represented by a solvent mixture of pH 3.3 and water (93:7, *v*/*v*), flowed through the chromatographic system with a flow rate of 1.0 mL/min, in isocratic elution. A total of 10 µL of the sample to be separated was injected into the system, the run time lasted for 35 min per registered chromatogram, and the detection of the separated components was measured at 275 nm wavelength.

2.5.3. Mobile Phase Preparation

The mobile phase was comprised of 93% solvent A and 7% water R (of chromatographic use) (93:7, *v*/*v*), where solvent A was prepared by mixing water R and acetonitrile R (20 80, *v*/*v*), 0.7 mL triethylamine R added, and the pH adjusted to 3.3 with orthophosphoric acid R. The obtained solution was filtered and sonicated for around one hour before use.

2.5.4. Samples Preparation

The compounds **1h**, **1j**, **1i**, **1m**, **1g,** and **1n** were intended to be separated from the mixture. Challenges regarding their close chemically related structures, their purity, and difficulty in eluting one component at a different time point were considered and the current analytical method was developed to overcome the issue.

System Suitability

A test solution that contained 5 µg/mL from each of the components was injected into the chromatographic system, following the optimized chromatographic conditions, and the retention time of the main peaks due to tested compounds, resolution, theoretical plates, and symmetry factors were evaluated.

Individual stock solutions of 500 µg/mL were prepared from every tested chemical substance (**1h**, **1j**, **1i**, **1m**, **1g**, and **1n**). An amount of 5 mg was transferred into a 10 mL volumetric flask, 5 mL acetonitrile R was added, and the flask was sonicated for 5 min, cooled to room temperature, and diluted to volume with acetonitrile R. The final test solution was obtained by diluting 0.25 mL from each stock solution to 25 mL with methanol R, leading to a concentration of 5 µg/mL from each of the compounds **1h**, **1j**, **1i**, **1m**, **1g**, and **1n**.

Specificity

To evaluate the specificity of the method, individual solutions of 5 µg/mL from each chemical entity were injected, along with the diluent. The identification solutions were prepared firstly by obtaining stock solutions of 500 µg/mL in acetonitrile R, followed by their dilution of 0.25 mL to 25 mL with methanol R, to reach the concentration of 5 µg/mL.

The interference of diluent in the identification of compounds **1h**, **1j**, **1i**, **1m**, **1g**, and **1n** was evaluated.

LOD—LOQ

The limits of detection (LOD) and quantification (LOQ) address the ability of the method to detect and quantify low amounts of analytes in the samples. There are different approaches for LOD and LOQ calculation; currently, the parameters are determined statistically based on the calibration curve, using standard deviation (σ) and slope (S), as expressed in Equations (2) and (3) [29].

$$\mathrm{LOD} = \frac{3.3 \times \sigma}{\mathrm{S}} \quad (2)$$

$$\text{LOD} = \frac{10 \times \sigma}{\text{S}} \quad (3)$$

Increasingly concentrated solutions in the range of 0.06–0.5 μg/mL were prepared for each compound. Firstly, individual stock solutions were prepared from each solid dissolved in acetonitrile R, in a suitable amount to reach 500 μg/mL concentration. Furthermore, a cumulative stock solution of 4.0 μg/mL was obtained by diluting each stock solution to a specific volume with methanol R. The desirable number of concentrations was obtained by dilution of cumulative stock solution (the detailed preparation of concentration ranges is included in the Supplementary Materials—RP-HPLC Analytical Report and Chromatograms, LOD and LOQ chapters).

The calibration plot that sustained the linear relationship between the area under registered peaks and their concentrations was traced. A linear calibration curve is described by a regression model, a correlation coefficient ($R^2 \geq 0.99$), standard deviation, and slope of the line.

Linearity

As per Q2(R1) [30], the linearity represents the capacity to obtain results directly proportional to the concentration of the analyte in the prepared sample solution.

A linear calibration curve is a positive indication of analytical method performance in a specific concentration range.

The linear relationship between the concentration (X-axis) of the analyte and the response (Y-axis) was plotted. The obtained calibration curve was evaluated in terms of correlation coefficient ($R^2 \geq 0.99$), slope, and y-intercept.

For the current analytical method, the linearity was studied from the reporting level of each chemical to 120% of the established concentration. Specifically, the method has been tested for linearity in a range of theoretical working concentrations: LOQ—6 μg/mL (0.06 μg/mL, 0.08 μg/mL, 0.1 μg/mL, 0.2 μg/mL, 0.5 μg/mL, 4.0 μg/mL, 5.0 μg/mL, 6 μg/mL). The successive dilutions were prepared from stock solutions of 500 μg/mL, using acetonitrile R as solvent. The desired concentrations were obtained by suitable dilutions in methanol R (the detailed preparation of concentration ranges is included in the Supplementary Materials—RP-HPLC Analytical Report and Chromatograms, Linearity chapter).

Precision

The precision of the analytical method has been demonstrated by intra-assay and intermediate precision.

Six solutions of 5.0 μg/mL **1h**, **1j**, **1i**, **1m**, **1g**, and **1n** each were prepared, injected in the chromatographic system, and registered on two consecutive days, then evaluated for relative standard deviation. The solutions were prepared from stock solutions of 500 μg/mL, with acetonitrile R used as a solvent. To reach 5.0 μg/mL concentration, dilutions in methanol R were realized (extensive preparation of the solutions is included in the Supplementary Materials—RP-HPLC Analytical Report and Chromatograms, Precision chapter).

Accuracy

An accuracy study was developed by preparing increasingly concentrated solutions of analytes in the range of 4–6 μg/mL (considering 4 μg/mL at the level of 80%, 5 μg/mL–100%, 6 μg/mL–120%). For each concentration level, six solutions were prepared and analyzed (extensive preparation of the solutions can be consulted in the Supplementary Materials—RP-HPLC Analytical Report and Chromatograms, Accuracy chapter). The determined and theoretical concentrations were calculated and the recovery was determined, along with the confidence interval.

Robustness

The parameters altered to demonstrate the robustness of the method were chosen concerning the percentage of mobile phase (solvent A: solvent B, 91:9, *v*/*v*, and solvent A: solvent B, 95:5, *v*/*v*), flow rate (±0.2 mL/ min), and column temperature (35 °C).

The variations were made from the validated chromatographic conditions: mobile phase = Solvent A: Solvent B (93:7, *v*/*v*), flow rate = 1.0 mL/min, column temperature = room temperature.

The robustness was checked based on a solution of 5.0 µg/mL **1h**, **1j**, **1i**, **1m**, **1g**, and **1n** each, prepared according to the RP-HPLC Analytical Report and Chromatograms, Robustness chapter, enclosed in the Supplementary Materials.

The effect of variations has been examined in terms of the retention time of the main peaks, and resolution.

3. Results

3.1. Chemistry

The condensation between different acid chlorides with ammonium thiocyanate and the reaction of isothiocyanates as key intermediates obtained in situ, with amines, is one of the most frequently used synthetic routes to obtain the *N*-acyl thiourea derivatives.

Thus, the new compounds (**1a**–**1o**) resulted from treating 2-((4-ethylphenoxy)methyl)benzoyl isothiocyanate (2) with a heterocyclic amine. The isothiocyanate was obtained in the reaction of 2-((4-ethylphenoxy)methyl)benzoic acid chloride (3) with ammonium thiocyanate.

The acid chloride (3) was prepared by refluxing 2-((4-ethylphenoxy)methyl)benzoic acid (4) with thionyl chloride in a dichloroethane medium. The acid (4) resulted from acidification with a mineral acid of the corresponding potassium salt (5), which in turn resulted from phthalide (6) and 4-ethylphenol.

The preparation of the new derivatives is described in Scheme 1.

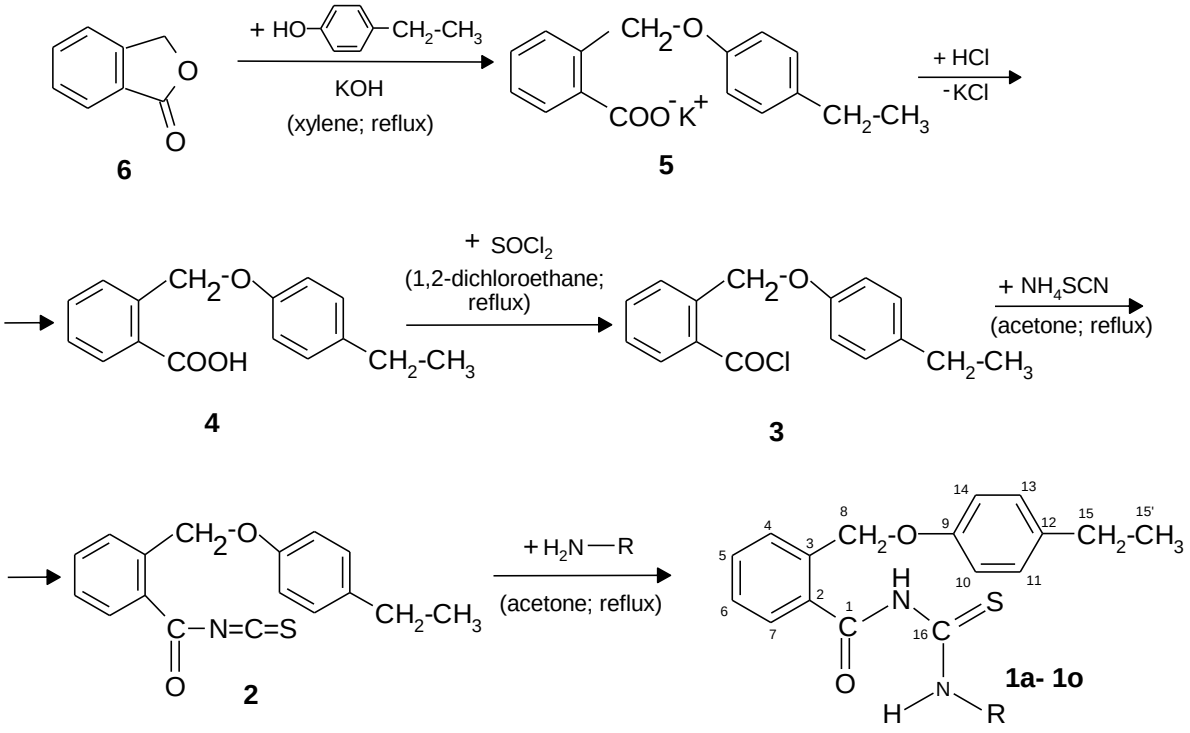

Scheme 1. *Cont.*

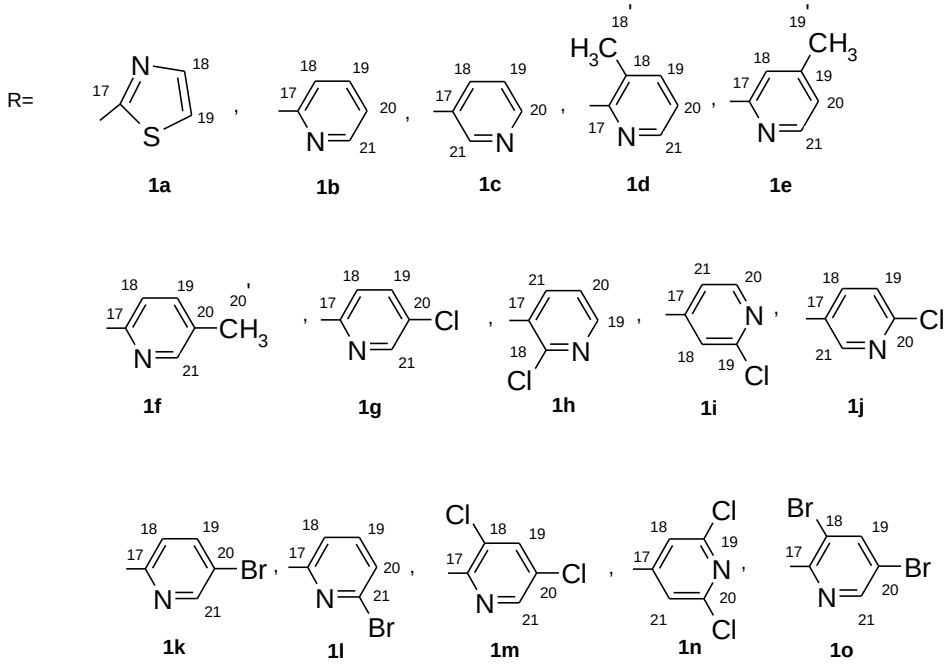

Scheme 1. Synthesis scheme of new *N*-acyl thiourea derivatives.

3.2. Spectral Data

Spectral methods confirmed the chemical structure of the new compounds: Fourier transform infrared (FT-IR), nuclear magnetic resonance (NMR), and atmospheric pressure chemical ionization (APCI) mass spectrometry (MS).

In the **1h**-NMR spectra, the -NH protons resonated as singlets or broad singlets in the range of 12.11–13.08 ppm and 11.82–12.60 ppm. The -CH2-O- protons signal was observed in the region 5.26–5.28 as a singlet. The ethyl group protons appear as a triplet at 1.08–1.14 ppm for -CH3 group, and as a quartet at 2.47–2.53 ppm for -CH2- group.

In the ^{13}C-NMR, the C=O and C=S carbons gave signals in the regions 166.72–170.28 ppm, and 177.47–180.54 ppm, respectively. The methylene carbon of -CH2-O group appears in the range of 67.29-67.56 ppm and the ethyl group carbons appear at 15.52–15.79 ppm (-CH3) and 27.16–27.25 ppm (-CH2-).

APCI+ high-resolution mass spectra were recorded for all compounds in a mixture of DMSO and MeOH. The molecular peaks $[M + H]^+$ were observed as base peaks for ten compounds out of fifteen (**1b**, **1c**, **1e**, **1f**, **1g**, **1i**, **1j**, **1l**, **1n**, and **1o**), thus confirming the identity of the investigated species. For **1h**, the base peak is corresponding to the $[M - Cl]^+$ cation. In the mass spectra of compounds **1a**, **1d**, **1k**, and **1m**, the base peak is related to the $[C_{16}H_{15}O_2]^+$ fragment (calculated m/z 239.10666), whose structure is depicted on the scheme below (Figure 1). Other frequently observed peaks in the mass spectra correspond to the $[C_{16}H_{18}NO_2]^+$ and $[C_8H_8NO]^+$ cations at calculated m/z values of 256.13321 and 134.06004, whose structures are drawn in Figure 1.

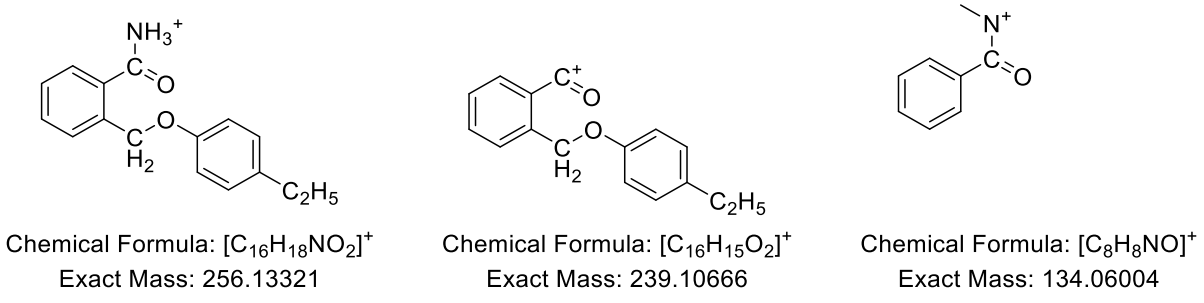

Figure 1. Cations depicted in the mass spectra.

3.3. Biological Evaluation of the Antimicrobial Activity

The results of the quantitative evaluation of the antimicrobial activity of the analyzed compounds are presented in Table 1. The MIC values, determined against the two Gram-negative bacteria: *E. coli* ATCC 25922 and *P. aeruginosa* ATCC 27853, and Gram-positive bacteria: *S. aureus* ATCC 25923 and *E. faecalis* ATCC 29212, ranged from 2500 to 625 μg/mL, indicating that the compounds exhibited low antimicrobial activity, as compared to the positive control represented by ciprofloxacin (MICs values of 0.012–0.62 μg/mL).

Table 1. The MICs values (μg/mL) obtained for the tested compounds.

Strain/ Compound	*Staphylococcus aureus* ATCC 25923	*Enterococcus faecalis* ATCC 29212	*Escherichia coli* ATCC 25922	*Pseudomonas aeruginosa* ATCC 27853
1a	625	1250	1250	1250
1b	1250	1250	1250	1250
1c	1250	1250	1250	1250
1d	1250	1250	1250	1250
1e	1250	1250	1250	1250
1f	2500	2500	1250	1250
1g	625	1250	1250	625
1h	625	1250	1250	1250
1i	1250	1250	2500	1250
1j	2500	1250	1250	2500
1k	2500	1250	1250	1250
1l	2500	1250	2500	2500
1m	2500	1250	1250	1250
1n	1250	1250	1250	1250
1o	625	1250	2500	1250
Standard Deviation	776	323	518	484
Ciprofloxacin	0.15	0.62	0.01	0.15

Regarding the influence of the obtained compounds on bacterial adherence, the results showed a low antibiofilm activity, by comparison with the antibiotic control, with MBICs values of >5000–312 μg/mL (results attached in Table 2).

Table 2. The MBICs values (μg/mL) obtained for the tested compounds.

Strain/ Compound	*Staphylococcus aureus* ATCC 25923	*Enterococcus faecalis* ATCC 29212	*Escherichia coli* ATCC 25922	*Pseudomonas aeruginosa* ATCC 27853
1a	625	1250	1250	1250
1b	2500	1250	1250	1250
1c	2500	1250	1250	1250
1d	1250	1250	1250	1250
1e	1250	1250	312	1250
1f	2500	2500	1250	1250
1g	625	1250	625	1250
1h	1250	1250	1250	1250
1i	2500	1250	1250	1250
1j	2500	1250	2500	2500
1k	2500	1250	1250	2500
1l	2500	1250	1250	2500
1m	2500	1250	1250	2500
1n	>5000	>5000	1250	>5000
1o	1250	625	1250	625
Standard Deviation	1100	1026	449	1079
Ciprofloxacin	0.15	0.62	0.012	0.15

3.4. Total Antioxidant Capacity Measurements

The total antioxidant capacity (TAC) was measured using the well-known DPPH method, as mentioned previously. Ascorbic acid was used as a reference, with a determined antioxidant capacity of 100%. The obtained results are shown in Table 3. The highest antioxidant capacity was recorded for the compound **1i** (87%), followed by **1a** (44%), while for the other compounds, TAC values were between 0 and 29%. The TAC value of every compound was calculated with regard to the antioxidant capacity of the reference (ascorbic acid, TAC = 100%).

Table 3. TAC values (%) for compounds **1a**–**1o**.

Compound	1a	1b	1c	1d	1e	1f	1g	1h	1i	1j	1k	1l	1m	1n	1o
TAC (%)	44	1	10	0	0	11	16	9	87	22	21	20	21	24	29

3.5. Analytical Method Validation by PR-HPLC Technique

3.5.1. Specificity

The system suitability of the analytical method was inspected by monitoring the asymmetry of chromatographic peaks, their reasonable separation, along with the purity and theoretical plates. Methanol as a diluent was used for sample preparation and individual solutions of 5 µg/mL compounds **1h**, **1j**, **1i**, **1m**, **1g**, and **1n** were injected in the chromatographic system. The retention time and UV spectra were extracted for peak identification (Figure 2).

A solution that contained 5 µg/mL of each of the related compounds (**1h**, **1j**, **1i**, **1m**, **1g**, and **1n**) was injected, the chromatogram registered (Figure 3), and the peaks evaluated for system suitability parameters (the checked chromatogram was extracted from linearity validation parameter, solution 5 µg/mL **1h**, **1j**, **1i**, **1m**, **1g**, and **1n**).

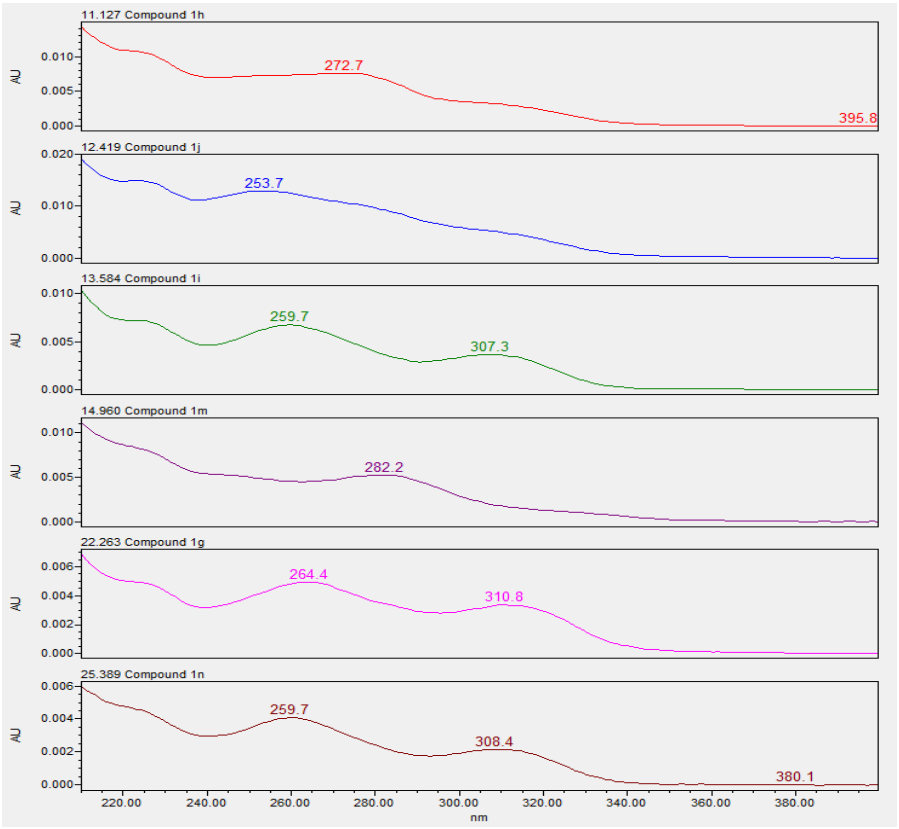

Figure 2. UV spectra of the chemical compounds **1h**, **1j**, **1i**, **1m**, **1g**, and **1n**.

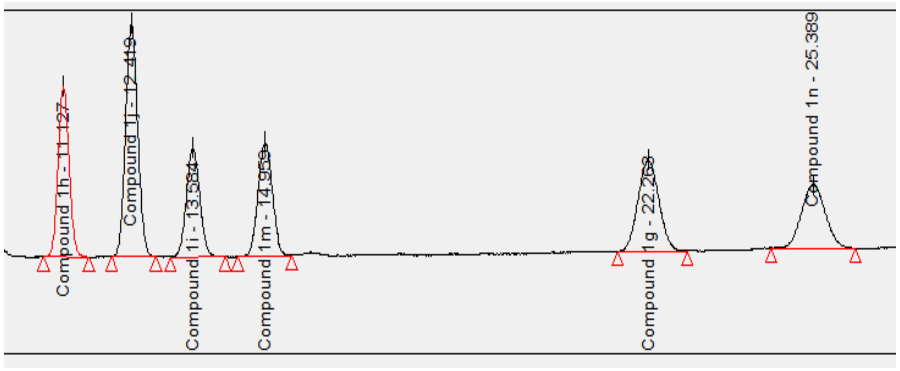

Figure 3. Typical chromatogram depicting **1h**, **1j**, **1i**, **1m**, **1g**, and **1n** peaks, for the proposed RP-HPLC separation method, linearity validation parameter (in extenso chromatograms attached to the validation parameters, along with the information regarding the nature of the chromatographic peaks are enclosed in the Supplementary Materials—RP-HPLC Reports and Chromatograms, Figures S2–S11).

For every compound revealed on the chromatogram, the symmetry factor (tailing factor) was in the range of 1.02–1.07, confirming the Gaussian symmetry of the peaks [31]. The degree of separation was checked through resolution; the chromatographic peaks were fully separated, as the resolution between two adjacent peaks proved to be greater than 2 [32]. Moreover, as the purity angle (PA) had values lower than the purity threshold (TH), the peak purity was confirmed. The theoretical plates (N) are a measure of column efficacy [33]; for every peak, the plate count was more than 11,000 (Table 4).

The interference study aims to demonstrate the lack of interference between the solvent used at solution preparation and the main peaks on the chromatogram. Figures 4 and 5 are typical HPLC chromatograms that demonstrate no interference between diluent and eluted compounds.

Table 4. System suitability parameters for the proposed and optimized method.

Parameter	Compounds Evaluated for System Suitability Conditions					
	1h	**1j**	**1i**	**1m**	**1g**	**1n**
Retention time (RT, min)	11.127	12.419	13.584	14.959	22.263	25.389
Symmetry factor (T)	1.07	1.07	1.07	1.04	1.04	1.08
Plate count (N)	13.020	13.614	13.362	13.633	14.879	14.817
Purity angle (PA)	0.314	0.187	0.438	0.457	0.528	0.721
Purity threshold (TH)	0.788	0.563	0.973	0.971	1.117	1.429
Resolution (R)	–	3.17	2.61	2.81	11.70	3.96

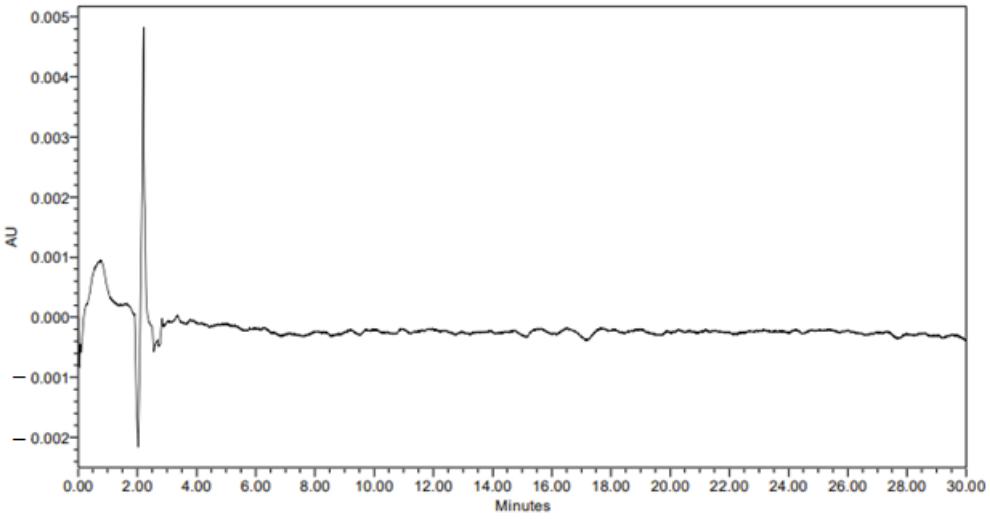

Figure 4. Chromatogram registered with the solvent used for samples preparation (methanol).

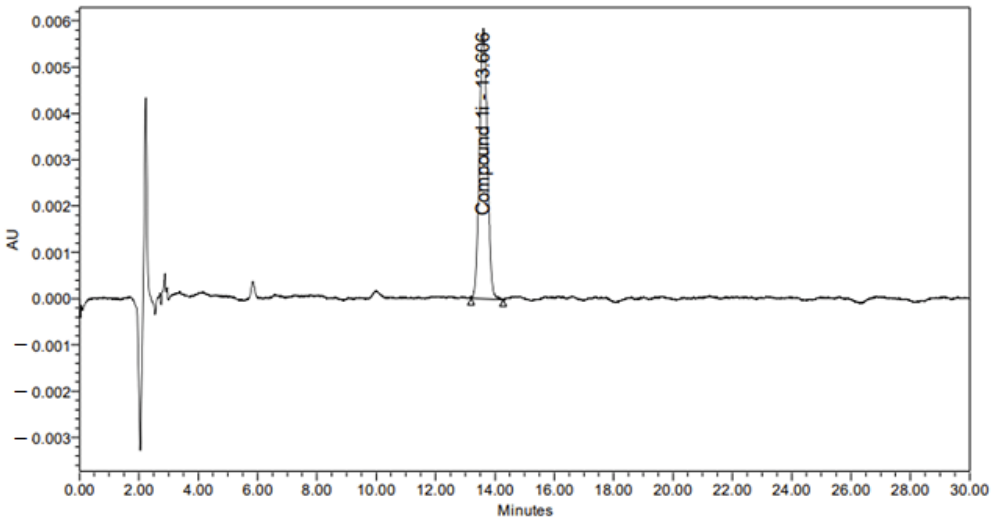

Figure 5. Chromatogram registered with 5 μg/mL **1i** solution.

The results sustain the hypothesis that the optimized analytical RP—HPLC method is well suited for the proper separation of the chemically related compounds **1h**, **1j**, **1i**, **1m**, **1g**, and **1n**.

3.5.2. LOD and LOQ

The calibration curve was traced by preparing increasingly concentrated solutions for every related compound, in the range of 0.06 μg/mL–0.5 μg/mL.

As mentioned, the calibration curve was described by a linear regression equation, where a linear relationship between the areas under the curve and their corresponding concentrations was proved by a correlation coefficient (R^2) greater than 0.99, for each series of solutions (the calibration plots for the related compounds are attached in the Supplementary Materials—HPLC Reports, along with the extensive description of solutions' preparation). LOD and LOQ values were estimated by regression analysis, considering the standard deviation and slope, calculated for every plot (Table 5, Figure 6).

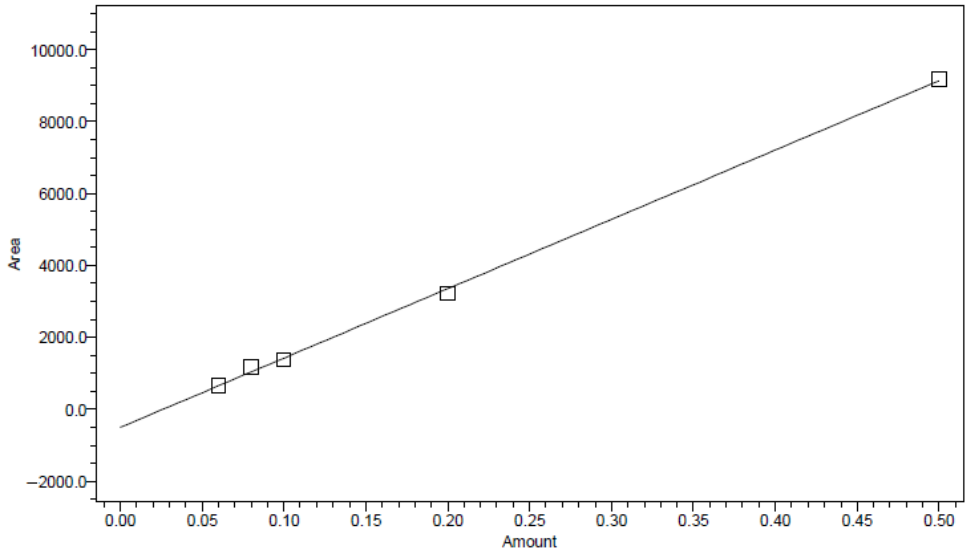

Figure 6. LOD—LOQ calibration curve (amount in μg/mL, area in atomic units) for **1i** increasingly concentrated solutions; where slope (b) = 19265.90, standard deviation = 118.33, coefficient of linear regression (R^2 = 0.99915). The calibration plot was extracted from HPLC Empower 3 Software (extensive data and chromatograms are attached to the Supplementary Materials section, Table S5, Figure S12).

Table 5. LOD-LOQ results for compounds **1h**, **1j**, **1i**, **1m**, **1g**, and **1n**, expressed in μg/mL and % (considering 100% a solution of 5 μg/mL of each tested compound).

Compound	STDEV (σ)	SLOPE (S)	LOD		LOQ	
			μg/mL	%	μg/mL	%
1h	181.72	23750.89	0.0252	0.504	0.0765	1.530
1j	183.68	26862.68	0.0205	0.410	0.0684	1.368
1i	118.33	19265.90	0.0184	0.368	0.0614	1.228
1m	139.32	18696.35	0.0224	0.448	0.0745	1.490
1g	127.23	16188.43	0.0236	0.472	0.0786	1.572
1n	110.25	13827.25	0.0239	0.478	0.0797	1.594

For the investigated compounds, the limit of detection was set in the range 0.0184 μg/mL–0.0252 μg/mL, while the limit of quantification was within 0.0614 μg/mL–0.0797 μg/mL. The method based on the dispersion characteristics of the regression line [34,35] was able to point out the lowest distinguishable and the lowest quantifiable concentrations of the chemicals.

3.5.3. Linearity

For the linearity parameter, the regression line was traced in the concentration range of 0.06–6.00 μg/mL. The linear relationship between concentration and response was demonstrated for every compound, by a correlation coefficient (R^2) greater than 0.99 (Table 6, Figure 7).

Table 6. The characteristics of regression lines that demonstrate the linearity of the method for the compounds **1h**, **1j**, **1i**, **1m**, **1g**, and **1n.**

Compound	STDEV (σ)	SLOPE (S)	Correlation Coefficient ($R^2 \geq 0.99$)
1h	383.40	22,233.20	0.999961
1j	1191.98	33,754.45	0.999836
1i	673.52	17,156.19	0.999797
1m	541.35	19,734.90	0.999901
1g	1147.85	22,536.96	0.999658
1n	957.13	18,315.26	0.999640

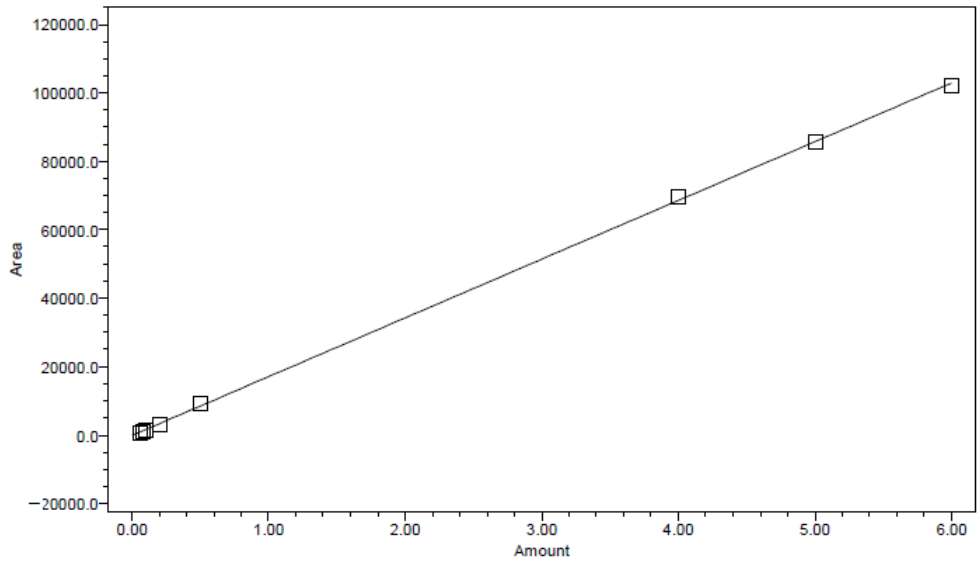

Figure 7. A linearity calibration curve (amount in μg/mL, area in atomic units) for **1i** increasingly concentrated solutions; where slope (b) = 17156.19, standard deviation = 673.52, coefficient of linear regression (R^2 = 0.999797). The calibration plot was extracted from HPLC Empower 3 Software (extensive data and chromatograms are attached to the Supplementary Materials section, Table S6, Figure S13).

3.5.4. Precision Results

Precision is defined as the degree of proximity among a set of results.

Six samples were prepared to determine the intra-assay precision (Tables 7 and 8), while for the intermediate precision that measured the precision of the analytical method, six samples were prepared on two different days (Table 9). The precision of the results was evaluated by the relative standard deviation (RSD) values in the series of measurements. RSD values < 2.0% were recorded in every scenario, proving the precision of the analytical method.

Table 7. Precision results for compounds **1h**, **1j**, **1i**, **1m**, **1g**, **1n**–5 μg/mL solution—first day.

Precision (I) Results for Compounds 1h, 1j, 1i, 1m, 1g, 1n–5 μg/mL Solution												
Sample No.	Compound 1h		Compound 1j		Compound 1i		Compound 1m		Compound 1g		Compound 1n	
	Ret. Time (min.)	Peak Area (μV × sec)	Ret. Time (min.)	Peak Area (μV × sec)	Ret. Time (min.)	Peak Area (μV × sec)	Ret. Time (min.)	Peak Area (μV × sec)	Ret. Time (min.)	Peak Area (μV × sec)	Ret. Time (min.)	Peak Area (μV × sec)
1.	11.270	111,591	12.596	169,135	13.789	82,009	15.167	97,170	22.721	108,491	25.932	84,215
2.	11.272	111,110	12.602	168,465	13.801	82,735	15.168	96,179	22.742	109,245	25.950	84,630
3.	11.276	111,024	12.612	168,231	13.818	82,661	15.178	96,381	22.766	108,577	25.974	82,741
4.	11.281	110,663	12.614	168,785	13.816	82,849	15.190	95,668	22.768	107,246	25.991	83,968
5.	11.286	110,997	12.620	169,796	13.824	82,632	15.196	97,012	22.779	108,996	26.003	84,959
6.	11.293	110,417	12.632	166,835	13.836	82,261	15.197	96,243	22.789	106,276	26.013	83,531
Average	11.280	110,967	12.613	168,541	13.814	82,525	15.183	96,442	22.761	108,138	25.977	84,007
(1) SD	0.009	402	0.013	1000	0.017	321	0.014	560	0.025	1144	0.031	796
(2) RSD %	0.08	0.36	0.10	0.59	0.12	0.39	0.09	0.58	0.11	1.06	0.12	0.95

(1) Standard deviation; (2) Relative standard deviation, %.

Table 8. Precision results for compounds **1h**, **1j**, **1i**, **1m**, **1g**, **1n**–5 μg/mL solution—second day.

Precision (II) Results for Compounds 1h, 1j, 1i, 1m, 1g, 1n–5 μg/mL Solution												
Sample No.	Compound 1h		Compound 1j		Compound 1i		Compound 1m		Compound 1g		Compound 1n	
	Ret. Time (min)	Peak Area (μV × sec)	Ret. Time (min.)	Peak Area (μV × sec)	Ret. Time (min.)	Peak Area (μV × sec)	Ret. Time (min.)	Peak Area (μV × sec)	Ret. Time (min.)	Peak Area (μV × sec)	Ret. Time (min.)	Peak Area (μV × sec)
1.	11.142	110,842	12.456	168,780	13.649	80,744	15.006	97,663	22.563	106,865	25.801	83,077
2.	11.330	109,970	12.672	166,002	13.886	79,884	15.250	97,797	22.896	106,337	26.148	81,794
3.	11.306	109,387	12.646	165,117	13.853	79,171	15.209	96,058	22.831	104,014	26.056	82,753
4.	11.281	114,244	12.615	172,220	13.805	81,127	15.179	98,678	22.722	108,103	25.945	80,985
5.	11.261	111,967	12.585	166,791	13.783	82,099	15.138	98,075	22.681	108,183	25.875	84,121
6.	11.245	108,129	12.562	163,043	13.749	77,962	15.126	94,606	22.594	103,635	25.773	79,668
Average	11.261	110,757	12.589	166,992	13.787	80,164	15.151	97,146	22.714	106,189	25.933	82,066
(1) SD	0.066	2147	0.076	3183	0.084	1478	0.085	1519	0.131	1968	0.147	1594
(2) RSD %	0.58	1.94	0.61	1.91	0.61	1.84	0.56	1.56	0.57	1.85	0.57	1.94

(1) Standard deviation; (2) Relative standard deviation, %.

Table 9. Intermediate precision results for compounds **1h**, **1j**, **1i**, **1m**, **1g**, **1n**–5 μg/mL solution.

Intermediate Precision Results for Compounds 1h, 1j, 1i, 1m, 1g, 1n–5 μg/mL Solution												
Sample No.	Compound 1h		Compound 1j		Compound 1i		Compound 1m		Compound 1g		Compound 1n	
	Ret. Time (min)	Peak Area (μV × sec)	Ret. Time (min)	Peak Area (μV × sec)	Ret. Time (min.)	Peak Area (μV × sec)	Ret. Time (min)	Peak Area (μV × sec)	Ret. Time (min)	Peak Area (μV × sec)	Ret. Time (min)	Peak Area (μV × sec)
1.	11.270	111,591	12.596	169,135	13.789	82,009	15.167	97,170	22.721	108,491	25.932	84,215
2.	11.272	111,110	12.602	168,465	13.801	82,735	15.168	96,179	22.742	109,245	25.950	84,630
3.	11.276	111,024	12.612	168,231	13.818	82,661	15.178	96,381	22.766	108,577	25.974	82,741
4.	11.281	110,663	12.614	168,785	13.816	82,849	15.190	95,668	22.768	107,246	25.991	83,968
5.	11.286	110,997	12.620	169,796	13.824	82,632	15.196	97,012	22.779	108,996	26.003	84,959
6.	11.293	110,417	12.632	166,835	13.836	82,261	15.197	96,243	22.789	106,276	26.013	83,531
7.	11.142	110,842	12.456	168,780	13.649	80,744	15.006	97,663	22.563	106,865	25.801	83,077
8.	11.330	109,970	12.672	166,002	13.886	79,884	15.250	97,797	22.896	106,337	26.148	81,794
9.	11.306	109,387	12.646	165,117	13.853	79,171	15.209	96,058	22.831	104,014	26.056	82,753
10.	11.281	114,244	12.615	172,220	13.805	81,127	15.179	98,678	22.722	108,103	25.945	80,985
11.	11.261	111,967	12.585	166,791	13.783	82,099	15.138	98,075	22.681	108,183	25.875	84,121
12.	11.245	108,129	12.562	163,043	13.749	77,962	15.126	94,606	22.594	103,635	25.773	79,668
Average	11.270	110,862	12.601	167,767	13.801	81,345	15.167	96,794	22.738	107,164	25.955	83,037
(1) SD	0.046	1476	0.054	2390	0.059	1600	0.060	1152	0.093	1842	0.104	1572
(2) RSD %	0.40	1.33	0.43	1.42	0.43	1.97	0.40	1.19	0.41	1.72	0.40	1.89

(1) Standard deviation; (2) Relative standard deviation, %.

3.5.5. Accuracy Results

The accuracy of the analytical method was assessed by determining the degree of closeness between the real (theoretical) values of the analytes in the sample solutions and their determined concentrations. The accuracy parameter was performed for every compound, over three concentration levels, six replicates each (4 µg/mL–80%, 5 µg/mL–100%, 6 µg/mL–120%). Consequently, the accuracy was expressed as the percentage recovery of the determined amount of each analyte in the sample solutions, along with the relative standard deviations and confidence interval (Table 10 is an example of the calculus carried out to determine the recovery of the analyte **1i** at each level of concentration. For every tested compound, the accuracy results are filled in the Supplementary Materials, RP-HPLC Analytical Report and Chromatograms, Tables S7–S12). The recovery of each compound was determined, with results in a 95% confidence level. RSDs on the obtained results were in the range of 0.62–1.33%, meaning that the obtained recovery values were uniformly and tightly distributed around the mean.

Table 10. Accuracy levels—real (theoretical) and determined concentrations of compound **1i** and mean percent recovery (%) of six injections of each accuracy concentration (80%, 100%, and 120% analytical concentrations).

Sample No.	Accuracy Results for Compound 1i								
	4 µg/mL 1i Solution			5 µg/mL 1i Solution			6 µg/mL 1i Solution		
	Real (µg/mL)	Determined (µg/mL)	Recovery (%)	Real (µg/mL)	Determined (µg/mL)	Recovery, (%)	Real (µg/mL)	Determined (µg/mL)	Recovery, (%)
1.	4.0080	3.9700	99.05	4.9500	4.8641	98.26	5.9760	6.0261	100.84
2.	4.0080	4.0130	100.13	4.9500	4.9072	99.13	5.9760	6.0114	100.59
3.	4.0080	3.9996	99.79	4.9500	4.9028	99.05	5.9760	5.9827	100.11
4.	4.0080	3.9988	99.77	4.9500	4.9139	99.27	5.9760	6.0559	101.34
5.	4.0080	4.0086	100.01	4.9500	4.9011	99.01	5.9760	6.0050	100.48
6.	4.0080	3.8852	96.94	4.9500	4.8791	98.57	5.9760	6.0126	100.61
Average:			99.61						
Standard Deviation:			1.07						
Relative standard deviation (RSD%):			1.07						
Confidence interval (Probability 95%):			99.12–100.10						

3.5.6. Robustness Results

The robustness of the chromatographic method was evaluated by inducing deliberated variations in the method parameters. To provide evidence of the reliability of the method, alterations concerning mobile phase percentage, flow rate and column temperature were made and evaluated for a solution of 5 µg/mL **1h**, **1j**, **1i**, **1m**, **1g**, **1n** (Table 11). The resolution as a system suitability control parameter was checked in every tested scenario. As the resolution values proved to be more than 2, it was generally considered that the chromatographic peaks were completely separated and the developed analytical method is reliable and robust under the selected conditions.

Table 11. Robustness results for the proposed RP-HPLC analytical method.

Comp.	Validated Chromatographic Parameters [1]		Robustness—Deliberate Variations in Method Parameters –5 μg/mL Solution 1h, 1j, 1i, 1m, 1g, 1n									
			Mobile Phase Variation				Flow Rate Variation				Column Temperature Variation	
			Solvent A:Solvent B (91:9, *v*/*v*)		Solvent A:Solvent B (95:5, *v*/*v*)		Flow Rate 0.8 mL/min		Flow Rate 1.2 mL/min		Column Temperature 35 °C	
	Ret. Time (min)	Resolution [2]	Ret. Time (min)	Resolution [2]	Ret. Time (min)	Resolution [2]	Ret. Time (min)	Resolution [2]	Ret. Time (min)	Resolution [2]	Ret. Time (min)	Resolution [2]
1h	11.134	–	12.367	–	10.095	–	13.941	–	9.307	–	10.289	–
1j	12.430	3.23	13.947	3.49	11.169	2.96	15.571	3.46	10.393	3.06	11.384	3.10
1i	13.600	2.67	15.254	2.60	12.236	2.69	17.044	2.85	11.374	2.53	12.392	2.63
1m	14.969	2.82	16.984	3.18	13.317	2.50	18.751	2.99	12.510	2.64	13.733	3.20
1g	22.319	11.88	25.732	12.37	19.563	11.42	27.995	12.66	18.659	11.21	19.759	11.42
1n	25.466	4.05	29.367	4.16	22.208	3.87	31.927	4.28	21.292	3.83	22.509	4.19

[1] The method has been validated by setting the following chromatographic conditions: mobile phase = Solvent A: Solvent B (93:7, *v*/*v*), flow rate = 1.0 mL/min, column temperature = room temperature; [2] resolution calculated between couples of two successive peaks.

4. Discussion

The current research paper is a continuation of our previous efforts in this area [24], synchronizing with the current needs of novel antimicrobials to overcome the increasing resistance to accessible antibiotics. In this context, the study aimed to synthesize new *N*-acyl thiourea derivatives (referred to in the current paper as **1a**–**1o**), that incorporate both thiazole or pyridine nucleus in the same molecule. The present research is built on our previous in silico prediction and molecular docking studies, suggesting the antimicrobial potential of the designed compounds [24]. First, a series of molecular descriptors (area, volume, polar surface area, ovality, log P, polarizability, the energy of the frontier molecular orbitals) have been calculated based on the chemical structure of **1a**–**1o**, through in silico computational approaches, to predict their drug-like, absorption, distribution, metabolism, elimination, and toxicity (ADMET). According to Lipinski's rule, a promising chemical candidate with oral absorption and adequate permeability is characterized by a molecular mass not more than 500 Da, having maximum 10 H-bond acceptors, 5 H-bond donors and partition coefficient (log P) of 5 [36–38]. In the evaluated series, five compounds respected the Lipinski's rule of five (**1a**, **1b**, **1c**, **1e**, and **1f**), **1o** showed two violations (log P > 5, molecular mass > 500 Da), and the others showed one violation from the rule (log P > 5).

The biological activity of the studied compounds **1a**–**1o** has been previously checked through molecular docking studies [24]. The most favorable conformation of the ligands in the active site of receptor proteins (*S. aureus* DNA gyrase B and *E. coli* DNA gyrase B), has been confirmed by the presence of *H*-bonds established with the amino acid scaffolds of the selected receptors, and satisfactory docking scores. Consequently, the results obtained after generating the in silico studies provided an impetus to synthesize and evaluate the in vitro biological activities of chemicals **1a**–**1o**, on bacterial strains which are among the most threatening and challenging because of their resistance to all currently available antibiotics and high biofilm development ability. Among Gram-positive bacteria, *S. aureus* and *E. faecalis* are two of the most frequent Gram-positive opportunistic and nosocomial pathogens, exhibiting resistance to penicillin, methicillin, quinolones, aminoglycosides, macrolides, glycopeptides, and often harboring multi-drug resistance (MDR) phenotypes [39]. The Gram-negative bacilli, both glucose-fermentative (*E. coli*) and non-fermentative (*P. aeruginosa*), are involved in endogenous and exogenous infections that are very difficult to treat due to their multiple intrinsic and acquired resistance sometimes to the majority (extended-drug resistance) or even all tested antibiotics (pan-drug resistance), including last resorts such as plasmid-mediated colistin resistance [40,41]. The resistance determinants are often located on mobile genetic elements facilitating their escape from clinical settings to the community and the environment [42,43]. In addition to their genetic resistance, these opportunistic pathogens have also the ability to develop sessile communities on different tissues or implanted devices, and are very tolerant to high antibiotic concentrations. They are impossible to reach in vivo, thus inducing biofilm-associated infections, which are often hard to treat and lead to chronic, persistent conditions [44].

Among the tested compounds, **1a**, **1g**, **1h**, and **1o** had better activity in the series against *S. aureus* ATCC 25923, *P. aeruginosa* ATCC 27853 with moderate MIC values of 625 μg/mL.

The compound **1a** was designed with the thiazole ring on the backbone molecule. Structurally, thiazole has an electron-donating group (-S-) and an electron-accepting group (-C=N-). The thiazole nucleus demonstrated its activity against multi-drug resistant Gram-negative bacteria (*P. aeruginosa*) in recent studies [45,46].

The analogues substituted with halogens in the pyridine group showed similar antimicrobial activity against the tested bacterial strains. The derivatives designed with chlorine (**1g**: *5-chloro*; **1h**: *2-chloro*) and bromine (**1o**: *3,5-dibromo*) atoms on the pyridine ring distinguished in the series through higher activity. Thus, it may be inferred that the position of the halogen substituents improved the activity of the resulting compounds, in comparison with other designed isomers.

The moderate or low inhibition of the compounds may be the result of unsatisfactory penetration of the bacterial membrane. High log P results and/or the molecular mass can affect the bacterial membrane crossing [47]. Establishing a successful structure–activity relationship and the optimization of compound characteristics through the synthesis and analysis of a wider number of compounds remain focuses of compound design improvement that need to be addressed in the future, to induce better antibacterial activity.

From the tested compounds, **1e** exhibited the best antibiofilm activity against *E. coli* ATCC 25922, with an MBIC value of 312 μg/mL.

Remarkably, the compounds containing chlorine atoms in the molecule are designed as position isomers (i.e., **1g**, **1h**, **1i**, and **1j**; **1n** with **1m**). The relationship among compounds with respect to the chemical structure and their molecular properties inspired us to evaluate their similar chromatographic characteristics via the HPLC technique. In such cases of related substances, the phenomenon of peak co-elution becomes challenging. As the peak overlapping represents an issue in chromatography, in the current study, an RP-HPLC method is proposed and optimized to simultaneously separate and quantify the chemically related compounds **1g**, **1h**, **1i**, **1j**, **1n**, **1m**.

For the quantification of *N*-acyl-thiourea derivatives, we developed and reported a new RP-HPLC analytical method in a previous study [48]. The analysis was completed with an isocratic elution of 80% solvent A and 20% solvent B (*v*/*v*). Solvent A was represented by 6.8 g/L potassium dihydrogen phosphate R, while acetonitrile R, HPLC grade, represented solvent B. The method has also been validated and proved to be specific, precise, accurate, and linear in a particular range of concentrations, confirming that it is suited for the determination and quantification of 2-((4-methoxyphenoxy)methyl)-*N*-((6-methylpyridin-2-yl)carbamothioyl)benzamide.

Evaluating the data, both methods give similar results in terms of recovery (%), precision, and linearity. Despite these aspects, the newly developed and optimized method (as compared against the previously mentioned method) as well the increased simplicity of the experimental setup, i.e., the reduced number of steps for mobile phase preparation (water and acetonitrile R), the protection of the HPLC system by avoiding the use of phosphates for the mobile phase preparation and their precipitation during long analyses, the lower back pressure in the system, reduced consumption of reagents, and shorter turnaround time are reasons to support the use of the current optimized method for separation and quantification of the mentioned *N*-acyl-thiourea derivatives.

To demonstrate that the developed method fits its intended purpose, the validation parameters such as specificity, precision (intra-assay and intermediate precision), limits of detection (LOD) and quantification (LOQ), linearity, accuracy, and robustness have been completed, as per ICH guideline requirements [29]. The validation steps are described in the current study.

As for the specificity parameter, no interfering peaks were observed from the diluent. Although the peaks are closely chemically related, the chromatographic analytical method ensured their separation properly, avoiding a potential co-elution. The reasonable separation was sustained by resolution values higher than 2 between two consecutive peaks, along with the purity determination by purity angles < purity threshold.

The degree of repeatability was evaluated within the precision parameter. The results proved to be close to one another for six replicates of solutions (intra-assay precision), prepared on two different days (intermediate precision); specifically, the relative standard deviation values were less than 2, meeting the set acceptance criterion.

The lowest distinguished and determined concentration for every analyte in the sample was revealed by LOD—LOQ analysis, using dispersion characteristics of the regression line. For the six related compounds, the LOD limits were calculated in the range of 0.0184 μg/mL–0.0252 μg/mL, while LOQ ranged in an interval of 0.0614 μg/mL–0.0797 μg/mL. The linearity was demonstrated for each compound, covering the concentrations ranging from calculated LOQ to 6 μg/mL solutions of **1h**, **1j**, **1i**, **1m**, **1g**, and **1n**. Six regression lines corresponding to each analyte were traced for eight increasingly con-

centrated solutions. In every case, the analytes in the tested solutions proved to be linearly proportional to their concentration. The linearity was confirmed for every calibration plot, by evaluation of correlation coefficient, with satisfactory values ($R^2 \geq 0.999$).

The accuracy of the analytical procedure was determined over three concentration levels (80%, 100%, and 120% analytical concentrations), namely 4 μg/mL, 5 μg/mL, and 6 μg/mL solutions of **1h**, **1j**, **1i**, **1m**, **1g**, and **1n**. The standard deviation, relative standard deviation, and confidence interval were calculated for six replicate samples. The determined concentrations were reported as percent recovery of the known added amount of compound, as per ICH Q2(R1) and the results were within 98–102%.

By altering the parameters that may affect the analytical procedure, namely mobile phase composition, flow rate, and column temperature, the method proved to be robust and reliable during normal use.

The analytical method was found satisfactory for validation parameters, following ICH guidelines requirements. Hence, it can be routinely used for the simultaneous separation and quantification of compounds **1h**, **1j**, **1i**, **1m**, **1g**, and **1n** in a mixture.

5. Conclusions

The present study aimed to synthesize and characterize new *N*-acyl thiourea derivatives (**1a**–**1o**), incorporating both the thiazole or pyridine nucleus in the same molecule and showing a predicted antimicrobial potential previously studied by in silico approaches (the influence of electron-withdrawing, electron-donating atoms, and specific functional groups on the acyl thiourea moiety's heterocyclic core on the biological activities have been investigated).

After synthesis, the compounds have been physiochemically characterized by their melting points, IR, NMR, and MS spectra.

The in vitro evaluation of the antimicrobial activity has been performed against problematic opportunistic Gram-positive and Gram-negative bacterial strains (*Staphylococcus aureus*, *Enterococcus faecalis*, *Escherichia coli*, *Pseudomonas aeruginosa*) in planktonic (broth microdilution assay for the determination of the MIC values) and biofilm (crystal violet microtiter assay to establish the MBIC values) growth state. Among the tested compounds, **1a**, **1g**, **1h** and **1o** displayed better activity against planktonic *Staphylococcus aureus* and *Pseudomonas aeruginosa*, as revealed by the MIC values determined by the broth microdilution assay, while **1e** revealed the lowest antibiofilm activity against *Escherichia coli*.

The thiazole ring or the pyridine nucleus substituted with halogens (**1g***: 5-chloro;* **1h**: *2-chloro,* **1o***: 3,5-dibromo*), attached to the molecular backbone played a moderate role in inhibiting the microorganism's activity. The unsatisfactory inhibition of the microbial strains may be attributed to the poor penetration of the bacterial membrane. *N*-acyl thiourea derivatives may be the focus of further investigation, in which case, we aim to evaluate the molecular properties that impact the mechanism of action of the compounds against microbial strains, by designing a more advanced number of molecules so that the corroboration of the data can reach a statistically relevant estimation.

The total antioxidant activity (TAC), assessed by the DPPH method, evidenced the highest values for the compound **1i**, followed by **1a**.

Also, another purpose of our research was to optimize and validate a separation and quantification method for highly related compounds bearing a chlorine atom on the molecular backbone (**1g**, **1h**, **1i**, **1j**, **1m**, **1n**). To demonstrate that the developed method fits its intended purpose, the validation parameters such as specificity (no interfering peaks were observed from the diluent), precision (the relative standard deviation values were less than 2, meeting the set acceptance criterion), limits of detection (LOD) (calculated in the range of 0.0184–0.0252 μg/mL) and quantification (LOQ) (ranging in 0.0614–0.0797 μg/mL) interval, linearity (demonstrated for each compound, covering the concentrations ranging from calculated LOQ to 6 μg/mL solutions), accuracy (determined over three concentration levels, i.e., 80%, 100%, and 120% analytical concentrations, the results being within 98–102%), and robustness (demonstrated by altering mobile phase composition, flow rate, and

column temperature parameters) have been assessed and found satisfactory, according to ICH guideline requirements. Hence, the analytical method can be routinely used for the simultaneous separation and quantification of compounds **1h**, **1j**, **1i**, **1m**, **1g**, and **1n** in a mixture.

Supplementary Materials: The following supporting information can be downloaded at: https://www.mdpi.com/article/10.3390/pharmaceutics15102501/s1, RP-HPLC Analytical Report and Chromatograms: Figure S1: chromatogram registered with the solvent used for sample preparation (methanol); Figures S2a–S7a: chromatograms registered with 5 µg/mL solution of each compound; Figures S2b–S7b: UV spectra of each compound; Figure S8: 3D plot of compounds **1h**, **1j**, **1i**, **1m**, **1g**, and **1n**; Figure S9: typical chromatogram depicting **1h**, **1j**, **1i**, **1m**, **1g**, and **1n** peaks, for the proposed RP-HPLC separation method; Figure S10: UV spectra of the chemical compounds **1h**, **1j**, **1i**, **1m**, **1g**, and **1n**; Figure S11: identification chromatograms depicting **1h**, **1j**, **1i**, **1m**, **1g**, and **1n** peaks, registered following the proposed RP-HPLC separation method conditions; Figures S12a–f. LOD-LOQ calibration curves for **1h**, **1j**, **1i 1m**, **1g**, **1n**, amount in µg/mL; Figures S13a–f. linearity plots extracted from Empower 3 software, for **1h**, **1j**, **1i, 1m**, **1g**, **1n**;. Table S1: acceptance criteria for proposed analytical method; Tables S2–S4: precision results for compounds **1h**, **1j**, **1i**, **1m**, **1g**, **1n**–5 µg/mL solution–intra-assay and intermediate precision; Table S5: LOD-LOQ results for compounds **1h**, **1j**, **1i**, **1m**, **1g**, and **1n**, expressed in µg/mL and % (considering 100% a solution of 5 µg/mL of each tested compound); Table S6: linearity results for compounds **1h**, **1j**, **1i**, **1m**, **1g**, and **1n**; Tables S7–S12: accuracy levels—real (theoretical) and determined concentrations of each compound, and mean percent recovery (%) of six injections of each accuracy concentration (80%, 100%, and 120% analytical concentrations); Table S13: robustness results for the proposed RP-HPLC analytical method. ^{1h}-NMR and ^{13}C-NMR spectra for the compounds **1a**–**1o**: Figures S14–S43. IR spectra for the compounds **1a**–**1o**: Figures S44–S58.

Author Contributions: Conceptualization, R.R., L.P., D.C.N. and C.L.; methodology, R.R., L.P., D.C.N., M.T.C., F.D., I.Z., P.I., L.M., E.K. and C.L.; software, R.R., L.P. and E.K.; validation, R.R. and L.P.; formal analysis, R.R., L.P., D.C.N., M.T.C., F.D., I.Z., P.I., L.M., I.C.M., E.K., S.A. and C.L.; investigation, R.R., L.P., D.C.N., M.T.C., F.D., I.Z., P.I., I.C.M., L.M., E.K., S.A. and C.L.; resources, R.R., L.P., F.D., I.C.M., E.K., S.A. and C.L.; data curation, R.R., L.P., D.C.N., M.T.C., F.D., I.C.M., E.K. and C.L.; writing—original draft preparation, R.R.; writing—review and editing, R.R., L.P., D.C.N. and C.L.; visualization, R.R., L.P., D.C.N. and C.L.; supervision, L.P., D.C.N. and C.L.; project administration, R.R. and C.L.; funding acquisition, R.R. All authors have read and agreed to the published version of the manuscript.

Funding: Publication of this paper was supported by the University of Medicine and Pharmacy Carol Davila, through the institutional program Publish not Perish. This work was partially supported by "Carol Davila" University of Medicine and Pharmacy Bucharest, Romania through Contract no. 33PFE/30.12.2021 funded by the Ministry of Research and Innovation within PNCDI III, Program 1—Development of the National RD system, Subprogram 1.2—Institutional Performance—RDI excellence funding projects.

Institutional Review Board Statement: Not applicable.

Data Availability Statement: Not applicable.

Conflicts of Interest: The authors declare no conflict of interest. The company had no role in the design of the study; in the collection, analyses, or interpretation of data; in the writing of the manuscript, and in the decision to publish the results.

Abbreviation

Abbreviation list of words: ADMET (absorption, distribution, metabolism, elimination, toxicity); CFU (colony-forming units); DMSO (dimethyl sulfoxide); DPPH (2,2-diphenyl-1-picrylhydrazyl); ICH (International Council for Harmonisation of Technical Requirements for Registration of Pharmaceuticals for Human Use); IR (infrared); LOD (limit of detection); LOQ (limit of quantification); log P (partition coefficient); MBIC (minimum inhibitory concentration of the total biofilm mass development); MeOH (methanol); MIC (minimal inhibitory concentration); MS (mass spectrometry); N (theoretical plates); NMR (nuclear

magnetic resonance); PBS (phosphate buffer saline); PA (purity angle); TH (purity threshold); R (resolution); RP–HPLC (reversed-phase high-performance liquid chromatography); TAC (total antioxidant activity).

References

1. Hou, Y.; Zhu, S.; Chen, Y.; Yu, M.; Liu, Y.; Li, M. Evaluation of Antibacterial Activity of Thiourea Derivative TD4 against Methicillin-Resistant *Staphylococcus aureus* via Destroying the NAD+/NADH Homeostasis. *Molecules* **2023**, *28*, 3219. [CrossRef] [PubMed]
2. Özgeriş, B. Design, synthesis, characterization, and biological evaluation of nicotinoyl thioureas as antimicrobial and antioxidant agents. *J. Antibiot.* **2021**, *74*, 233–243. [CrossRef]
3. Lafzi, F.; Kilic, D.; Yildiz, M.; Saracoglu, N. Design, synthesis, antimicrobial evaluation, and molecular docking of novel chiral urea/thiourea derivatives bearing indole, benzimidazole, and benzothiazole scaffolds. *J. Mol. Struct.* **2021**, *1241*, 130566. [CrossRef]
4. Wan Zullkiplee, W.S.; Rasin, F.; Abd Halim, A.N.; Mortadza, N.A.; Ramli, N.; Hani, N.I.; Ngaini, Z. Synthesis, Biological Properties and Comparative Molecular Docking Evaluation Studies of 1,3 and 1,4 Bis-Thiourea Derivatives as Potential Antimicrobial Resistant Agents. *Int. J. Cur. Res. Rev.* **2021**, *3*, 23–30. [CrossRef]
5. Ghorab, M.M.; Alsaid, M.S.; El-Gaby, M.S.A.; Elaasser, M.M.; Nissan, Y.M. Antimicrobial and anticancer activity of some novel fluorinated thiourea derivatives carrying sulfonamide moieties: Synthesis, biological evaluation and molecular docking. *Chem. Cent. J.* **2017**, *11*, 32. [CrossRef] [PubMed]
6. Vedavathi, P.; Sudhamani, H.; Raju, C.N. Synthesis and antimicrobial activity of new urea and thiourea derivatives of (2′-(1*H*-tetrazol-5-yl)biphenyl-4-yl)methanamine. *Res. Chem. Intermed.* **2017**, *43*, 3251–3263. [CrossRef]
7. Channar, S.A.; Channar, P.A.; Saeed, A.; Alsfouk, A.A.; Ejaz, S.A.; Ujan, R.; Noor, R.; Bilal, M.S.; Abbas, Q.; Hussain, Z.; et al. Exploring thiazole-linked thioureas using alkaline phosphatase assay, biochemical evaluation, computational analysis and structure–activity relationship (SAR) studies. *Med. Chem. Res.* **2022**, *31*, 1792–1802. [CrossRef]
8. Abbas, S.Y.; Al-Harbi, R.A.K.; Sh El-Sharief, M.A.M. Synthesis and anticancer activity of thiourea derivatives bearing a benzodioxole moiety with EGFR inhibitory activity, apoptosis assay and molecular docking study. *Eur. J. Med. Chem.* **2020**, *198*, 112363. [CrossRef] [PubMed]
9. Arafa, W.A.A.; Ghoneim, A.A.; Mourad, A.K. N-Naphthoyl Thiourea Derivatives: An Efficient Ultrasonic-Assisted Synthesis, Reaction, and In Vitro Anticancer Evaluations. *ACS Omega* **2022**, *7*, 6210–6222. [CrossRef]
10. Stefanska, J.; Nowicka, G.; Struga, M.; Szulczyk, D.; Koziol, A.E.; Augustynowicz-Kopec, E.; Sanna, G. Antimicrobial and Anti-biofilm Activity of Thiourea Derivatives Incorporating a 2-Aminothiazole Scaffold. *Chem. Pharm. Bull.* **2015**, *63*, 225–236. [CrossRef]
11. Kondo, H.; Koshizuka, T.; Majima, R.; Takahashi, K.; Ishioka, K.; Suzutani, T.; Inoue, N. Characterization of a thiourea derivative that targets viral transactivators of cytomegalovirus and herpes simplex virus type 1. *Antiviral Res.* **2021**, *196*, 105207. [CrossRef]
12. Venkatachalam, T.; Qazi, S.; Samuel, P.; Uckun, F. Substituted heterocyclic thiourea compounds as a new class of anti-allergic agents inhibiting IgE/FcεRI receptor mediated mast cell leukotriene release. *Bioorg. Med. Chem.* **2003**, *11*, 1095–1105. [CrossRef]
13. Severina, H.; Skupa, O.; Voloshchuk, N.; Suleiman, M.; Georgiyants, V. Synthesis and anticonvulsant activity of 6-methyl-2-((2-oxo-2-arylethyl)thio)pyrimidin-4(3 *H*)-one derivatives and products of their cyclization. *Pharmacia* **2019**, *66*, 141–146. [CrossRef]
14. Çelen, A.; Kaymakçıoğlu, B.; Gümrü, S.; Toklu, H.; Arıcıoğlu, F. Synthesis and anticonvulsant activity of substituted thiourea derivatives. *Marmara Pharm. J.* **2011**, *15*, 043–047. [CrossRef]
15. Khokra, S.L.; Arora, K.; Khan, S.A.; Kaushik, P.; Saini, R.; Husain, A. Synthesis, Computational Studies and Anticonvulsant Activity of Novel Benzothiazole Coupled Sulfonamide Derivatives. *Iran J. Pharm. Res.* **2019**, *18*, 1–15. [PubMed]
16. Karakuş, S.; Koçyiğit-Kaymakçıoğlu, B.; Toklu, H.Z.; Arıcıoğlu, F.; Rollas, S. Synthesis and anticonvulsant activity of new N-(alkyl/substitutedaryl)-N′-[4-(5-cyclohexylamino)-1,3,4-thiadiazole-2-yl)phenyl]thioureas. *Arch. Pharm. Chem. Life Sci.* **2009**, *342*, 48–53. [CrossRef] [PubMed]
17. Thakur, A.S.; Ravitas, D.; Arvind, K.J.; Sudhir, K.P. Synthesis and Anticonvulsant Effect of Novel Thiazolidinedione Containing Benzene-sulfonylurea and Sulfonylthiourea Derivatives. *Cent. Nerv. Syst. Agents Med. Chem.* **2016**, *16*, 152–157. [CrossRef]
18. Naz, S.; Zahoor, M.; Umar, M.N.; Alghamdi, S.; Sahibzada, M.U.K.; UlBari, W. Synthesis, characterization, and pharmacological evaluation of thiourea derivatives. *Open Chem. J.* **2020**, *18*, 764–777. [CrossRef]
19. Singh, R.; Ganguly, S. Design, Synthesis and Evaluation of Some Novel 1-phenyl-3-(5-phenyl-1H-imidazol-1-yl) Thiourea Derivatives as Anti-HIV Agents. *Indian J. Pharm. Educ. Res.* **2018**, *52*, 655–665. [CrossRef]
20. Zahra, U.; Saeed, A.; Fattah, T.A.; Florke, U. Recent trends in chemistry, structure, and various applications of 1-acyl-3-substituted thioureas: A detailed review. *RSC Adv.* **2022**, *12*, 12710–12745. [CrossRef]
21. Maalik, A.; Rahim, H.; Saleem, M.; Fatima, N.; Rauf, A.; Wadood, A.; Riaz, M. Synthesis, antimicrobial, antioxidant, cytotoxic, antiurease and molecular docking studies of N-(3-trifluoromethyl) benzoyl-N′-aryl thiourea derivatives. *Bioorg. Chem.* **2019**, *88*, 102946. [CrossRef]
22. Keche, A.P.; Kamble, V.M. Synthesis and anti-inflammatory and antimicrobial activities of some novel 2-methylquinazolin-4(3H)-one derivatives bearing urea, thiourea and sulphonamide functionalities. *Arab. J. Chem.* **2019**, *12*, 1522–1531. [CrossRef]

23. Gülkok, Y.; Biçer, T.; Kaynak Onurdag, F.; Özgen, S.; Şahin, M.F.; Doğruer, D.S. Synthesis of some new urea and thiourea derivatives and evaluation of their antimicrobial activities. *Turk. J. Chem.* **2012**, *36*, 279–291. [CrossRef]
24. Roman, R.; Pintilie, L.; Nuță, D.; Avram, S.; Buiu, C.; Sogor, C.; Limban, C. In Silico Prediction, Characterization and Molecular Docking Studies on New Benzamide Derivatives. *Processes* **2023**, *11*, 479. [CrossRef]
25. Limban, C.; Missir, A.; Chiriță, I.C.; Nițulescu, G.M.; Ilie, C.; Căproiu, M.T. Some New 2-(4-Ethyl-phenoxymethyl)benzoic Acid Thioureides: Synthesis and Spectral Characterization. *Rev. Chim.* **2009**, *60*, 657–661.
26. Remes, C.; Paun, A.; Zarafu, I.; Tudose, M.; Caproiu, M.T.; Ionita, G.; Bleotu, C.; Matei, L.; Ionita, P. Chemical and biological evaluation of some new antipyrine derivatives with particular properties. *Bioorganic Chem.* **2012**, *41–42*, 6–12.
27. Paun, A.; Zarafu, I.; Caproiu, M.T.; Draghici, C.; Maganu, M.; Ionita, P.; Cotar, A.I.; Chifiriuc, M.C. Synthesis and evaluation of several benzocaine derivatives. *Comptes Rendus Chim.* **2013**, *16*, 665–671. [CrossRef]
28. Bem, M.; Baratoiu, R.; Radutiu, C.; Lete, C.; Mocanu, S.; Ionita, G.; Lupu, S.; Caproiu, M.T.; Madalan, A.M.; Patrascu, B.; et al. Synthesis and structural characterization of some novel methoxyamino derivatives with acid-basa and redox behavior. *J. Mol. Struct.* **2018**, *1173*, 291–299. [CrossRef]
29. ICH Guideline Q2(R2) on Validation of Analytical Procedures, EMA/CHMP/ICH/82072/2006. Available online: https://www.ema.europa.eu/en/documents/scientific-guideline/ich-guideline-q2r2-validation-analytical-procedures-step-2b_en.pdf (accessed on 19 June 2023).
30. ICH Topic Q2(R1). Validation of Analytical Procedures: Text and Methodology. Available online: https://www.ema.europa.eu/en/documents/scientific-guideline/ich-q-2-r1-validation-analytical-procedures-text-methodology-step-5_en.pdf (accessed on 22 June 2023.).
31. Stoll, D.R. Part 1: Basic Concepts in Peak Shape, and the Effect of Extracolumn Connections. *LC GC Eur.* **2021**, *34*, 315–318.
32. Barth, H.G. Chromatography Fundamentals, Part VIII: The Meaning and Significance of Chromatographic Resolution. *LC GC N. Am.* **2019**, *37*, 824–828.
33. Stauffer, E.; Dolan, J.A.; Newman, R. Gas Chromatography and Gas Chromatography—Mass Spectrometry. In *Fire Debris Analysis*; Elsevier: San Diego, CA, USA, 2008; pp. 235–293. [CrossRef]
34. Vial, J.; Jardy, A. Experimental comparison of the Different Approaches to Estimate LOD and LOQ of an HPLC Method. *Anal. Chem.* **1999**, *71*, 2672–2677. [CrossRef]
35. Mandrioli, M.; Tura, M.; Scotti, S.; Gallina Toschi, T.J.M. Fast detection of 10 cannabinoids by RP-HPLC-UV method in *Cannabis sativa* L. *Molecules* **2019**, *24*, 2113. [CrossRef]
36. Lipinski, C.A.; Lombardo, F.; Dominy, B.W.; Feeney, P.J. Experimental and computational approaches to estimate solubility and permeability in drug discovery and development settings. *Adv. Drug Deliv. Rev.* **1997**, *46*, 3–26. [CrossRef]
37. Saha, S.; Acharya, M. In silico ADME-toxicity profiling, prediction of bioactivity and CNS penetrating properties of some newer resveratrol analogues. *J. PharmaSciTech* **2014**, *3*, 98–105.
38. Bhal, S.K. *ACD/LogP—Making Sense of Value*; Advanced Chemistry Development, Inc.: Toronto, ON, Canada; Available online: www.acdlabs.com/logp/ (accessed on 13 July 2023).
39. Gheorghe, I.; Tatu, A.L.; Lupu, I.; Thamer, O.; Cotar, A.I.; Pircalabioru, G.G.; Chifiriuc, M.C. Molecular characterization of virulence and resistance features in *Staphylococcus aureus* clinical strains isolated from cutaneous lesions in patients with drug adverse reactions. *Rom. Biotechnol. Lett.* **2017**, *22*, 12321–12327.
40. Barbu, I.C.; Gheorghe-Barbu, I.; Grigore, G.A.; Vrancianu, C.O.; Chifiriuc, M.C. Antimicrobial Resistance in Romania: Updates on Gram-Negative ESCAPE Pathogens in the Clinical, Veterinary, and Aquatic Sectors. *Int. J. Mol. Sci.* **2023**, *24*, 7892. [CrossRef] [PubMed]
41. Truşcă, B.S.; Gheorghe-Barbu, I.; Manea, M.; Ianculescu, E.; Czobor Barbu, I.; Măruțescu, L.G.; Dițu, L.M.; Chifiriuc, M.C.; Lazăr, V. Snapshot of Phenotypic and Molecular Virulence and Resistance Profiles in Multidrug-Resistant Strains Isolated in a Tertiary Hospital in Romania. *Pathogens* **2023**, *12*, 609. [CrossRef] [PubMed]
42. Surleac, M.; Czobor Barbu, I.; Paraschiv, S.; Popa, L.I.; Gheorghe, I.; Marutescu, L.; Chifiriuc, M.C. Whole genome sequencing snapshot of multi-drug resistant Klebsiella pneumoniae strains from hospitals and receiving wastewater treatment plants in Southern Romania. *PLoS ONE* **2020**, *15*, e0228079. [CrossRef]
43. Marutescu, L.G.; Popa, M.; Gheorghe-Barbu, I.; Barbu, I.C.; Rodríguez-Molina, D.; Berglund, F.; Chifiriuc, M.C. Wastewater treatment plants, an "escape gate" for ESCAPE pathogens. *Front. Microbiol.* **2023**, *14*, 1193907. [CrossRef]
44. Vrancianu, C.O.; Serban, B.; Gheorghe-Barbu, I.; Czobor Barbu, I.; Cristian, R.E.; Chifiriuc, M.C.; Cirstoiu, C. The Challenge of Periprosthetic Joint Infection Diagnosis: From Current Methods to Emerging Biomarkers. *Int. J. Mol. Sci.* **2023**, *24*, 4320. [CrossRef] [PubMed]
45. Thakur, S.; Sharma, R.; Yadav, R.; Sardana, S. The Potential of Thiazole Derivatives as Antimicrobial Agents. *Chem. Proc.* **2022**, *12*, 36. [CrossRef]
46. Sharshira, E.M.; Cascioferro, S.M.; Parrino, B.; Carbone, D.; Schillaci, D.; Giovannetti, E.; Cirrincione, G.; Diana, P. Thiazoles, Their Benzofused Systems, and Thiazolidinone Derivatives: Versatile and Promising Tools to Combat Antibiotic Resistance. *J. Med. Chem.* **2020**, *63*, 7923–7956.

47. Shalas, A.F.; Winarsih, S.; Ihsan, B.R.P.; Kharismawati, A.; Firdaus, A.I.; Wiloka, E. Molecular docking, synthesis, and antibacterial activity of the analogs of 1-allyl-3-benzoylthiourea. *Res. Pharm. Sci.* **2023**, *18*, 371–380. [CrossRef] [PubMed]
48. Roman, R.; Pintilie, L.; Căproiu, M.T.; Dumitrașcu, F.; Nuță, D.C.; Zarafu, I.; Ioniță, P.; Chifiriuc, M.C.; Chiriță, C.; Moroșan, A.; et al. New N-acyl Thiourea Derivatives: Synthesis, Standardized Quantification Method and In Vitro Evaluation of Potential Biological Activities. *Antibiotics* **2023**, *12*, 807. [CrossRef] [PubMed]